This is the manuscript of the following published article:

T. Björninen, L. Sydänheimo, L. Ukkonen, Y. Rahmat-Samii, “Advances in antenna designs for UHF RFID tags mountable on conductive items,” *IEEE Antennas Propag. Mag.*, vol. 56, no. 1, Feb. 2014, pp. 79–103. DOI: 10.1109/MAP.2014.6821761



Published version is available in IEEE Xplore Digital Library:

http://ieeexplore.ieee.org/xpl/articleDetails.jsp?arnumber=6821761

# Advances in Antenna Designs for UHF RFID Tags Mountable on Conductive Items

Toni Björninen[1], Lauri Sydänheimo[1], Leena Ukkonen[1], Yahya Rahmat-Samii[2]

[1]Department of Electronics and Communications Engineering
Tampere University of Technology
Tampere, FI-33101, Finland
E-mail: toni.bjorninen@tut.fi, lauri.sydanheimo@tut.fi, leena.ukkonen@tut.fi

[2]Electrical Engineering Department
University of California, Los Angeles
Los Angeles, CA 90095, USA
E-mail: rahmat@ee.ucla.edu

***Abstract*—Design of antennas for metal mountable radio-frequency identification tags is driven by a unique set of challenges: cheap, small, low-profile and conformal structures need to provide reliable operation when tags are mounted on conductive platforms of various shapes and sizes. During the past decade, tremendous amount of research has been dedicated to meet these stringent requirements. Currently, the tag read ranges of several meters are achieved with flexible label type tags. Moreover, a whole spectrum of tag size-performance ratios has been demonstrated through a variety of innovative antenna design approaches. This article reviews and summarizes the progress made in antennas for metal mountable tags and presents future prospects.**

***Index Terms*—RFID, metal mountable tags, tag antennas, conformal antennas**

## I. Introduction

Passive radio-frequency identification (RFID) technology provides the automatic identification and tracking of items. This is achieved by labeling the items with battery-free remotely addressable tags composed of an antenna and an integrated circuit (IC). The use of propagating electromagnetic waves at ultra high frequencies (UHF) for powering and communicating with passive tags enables rapid interrogation of a large quantity of tags through various media from the distances of several meters. These are the main advantages that initially sparked the interest on passive UHF RFID systems [1][2]. Currently, they are used in access control, supply chain management, and in item-level asset tracking. The operation frequencies are regulated regionally within the sub-bands of the global frequency range of 840-960 MHz. A tutorial providing more details on the fundamentals of passive RFID systems is presented in the below inset.

Thanks to the versatility of passive RFID technology, new applications are continually emerging. For instance, RFID sensors based on antenna self-sensing and low-power integrated sensors have gained much attention [3][4]. The localization of tags and utilization of RFID in navigation of intelligent machines has been investigated [5][6]. Miniature, ultra-low-power and maintenance-free tags are also envisioned to provide platforms for wireless sensor nodes in the next generation internet − the internet of things [7][8]. Tracking of people with wearable garment-integrated tags [9] and a variety of bio-medical applications from detecting limb movement to miniature RFID-inspired neural recording tags are being investigated [10][11][12][13]. Fig. 1 illustrates the various practical applications of RFID.

The major factors driving the design and optimization of RFID tags are the stringent requirements on tag size, cost, and integration. Fundamental physical limitations exist on the achievable performance of an antenna with given size. Often, antennas occupying the spherical volume such that $ka \leq 0.5$, where $k=2\pi/\lambda$ is the free-space wavenumber and $a$ is the radius of a sphere circumscribing the maximum dimension of the antenna, are classified as electrically small [14]. For tag antennas, however, not only the volume, but also the thickness of the structure is strictly limited. This is because in most applications tags need to be inconspicuous. Thus, when considering the size-performance ratio of tag antennas, in addition to $ka$, it is also important to consider the antenna footprint and thickness separately.

To minimize the material and fabrication costs, tag antennas need to be impedance-matched by utilizing self-matching techniques (e.g. single and double T-matching, proximity-coupled loop feed, and parasitic loading [15][16][17][18]) to avoid the use of discrete components. This means, that the antenna geometry is adapted to provide the desired input impedance and radiation properties simultaneously. The modern computational electromagnetics tools are indispensable in tackling this challenge. [19][20]

Another special feature in the design of tag antennas is that

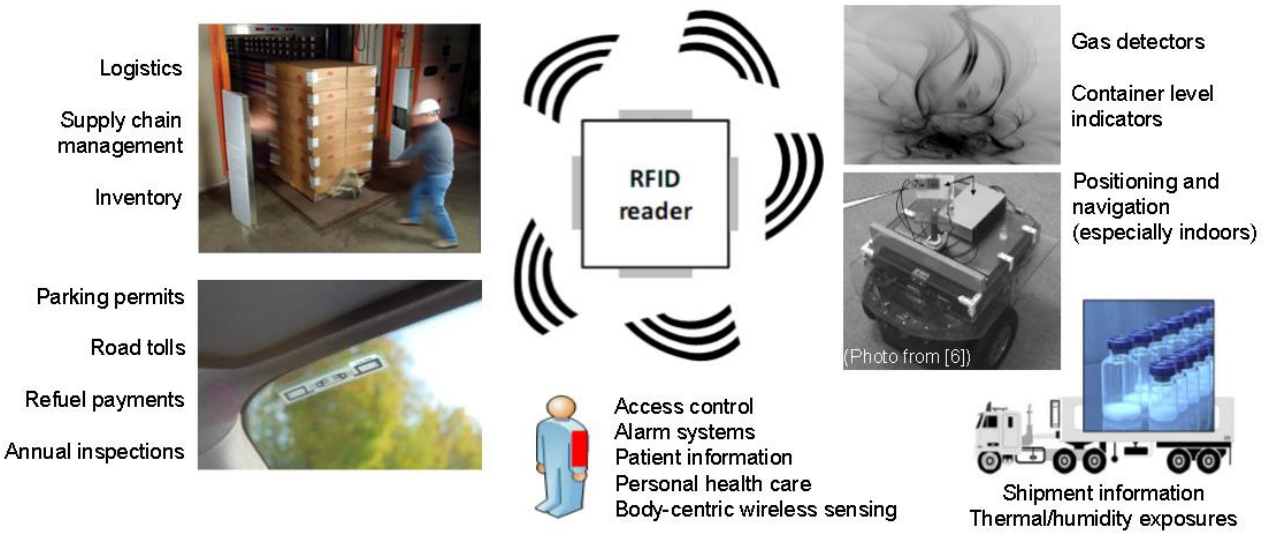


Fig. 1. Examples of applications of passive UHF RFID.

they need to be interfaced directly to an ultra-low-power RFID application specific integrated circuit (tag IC). The impedance of a tag IC is largely determined by the charge pump in the chip frontend [21]. It is a non-linear device and makes the IC impedance capacitive (example of a typical value: 15−j150 Ω). Therefore, the design of complex conjugate impedance matching for tag antennas is fundamentally different compared with conventional antennas which are commonly matched to 50 Ω. In particular, the accurate knowledge of the frequency-dependent tag IC impedance at the wake-up power of the chip is imperative for a successful design [22].

Finally, perhaps the greatest challenge yet to be overcome in the design of tag antennas is the undesired antenna-matter interaction, as in practice RFID tags are mounted on platforms with unspecified material properties. Thus, the development of antennas for low-profile and low-cost tags mountable on items containing or consisting of materials which have adverse effects on the functioning of conventional antennas is of paramount importance [23][24][25].

### A. *Challenge in Antennas for Metal Mountable Tags*

The undesired electromagnetic antenna-matter interaction is a particularly pronounced issue when tags are mounted on conductive items. The requirement of low-profile antenna structure leads to a situation where the separation of the antenna from a conductive surface is much less than a quarter wavelength. Hence, the antenna current flows predominantly horizontal to a conductive surface. In this configuration, the antenna operation is strongly influenced by the conductor [26]. Indeed, if the proximity of a conductive body is omitted in the design, the tag is likely not functional at all when mounted on a conductive item.

For dipole-like antennas, which are the most popular type of antennas used in RFID tags, this is explained by considering a line source parallel to a conductive plane. The electromagnetic boundary conditions require that the tangential electric field at the surface vanish. This means that there is a current on the surface with almost equal magnitude, but approximately opposite phase compared with the source current. Thus, the superposition of the radiation generated by the two current distributions approximately cancels out in the far field. Consequently, the antenna radiation efficiency will be low.

Alternatively, the image theory can be used to understand the phenomenon. In this case, an identical antenna (image source) is placed at an equal distance on the opposite side of the conductive plane which is assumed to have infinite extent. The plane is then removed, but its impact is modelled by feeding the image source antenna in such a way that the original boundary condition at the conductive plane is satisfied (the tangential electric field vanishes). This is achieved with an image source antenna carrying a current with equal magnitude but opposite phase compared with the primary source antenna. Theory of antenna arrays can then be used to find the far field radiation pattern. The computation of input impedance of the coupled antennas reveals that for very closely-spaced antennas the mutual resistance approaches the self-resistance [27]. This means that the coupled antennas become approximately short-circuited. Consequently, even small loss resistance will degrade the radiation efficiency. The antenna directivity, however, may be enhanced. In practice, the proximity of a conductive body (even a small one compared with the antenna) can greatly affect the antenna radiation pattern and the antenna impedance is a function of the distance to the metal [28]. Operation of a dipole antenna placed parallel to a conductive plane will be further studied in Section II.B.

Recalling the top priorities in the design of antennas for RFID tags; cheap and unobtrusive structure, it is evident that addressing jointly the fundamental limitations on antenna size-performance ratio and the adverse effects due the proximity of conductive bodies presents a prominent challenge. This makes it extremely difficult to achieve the high tag read ranges of several meters, while maintaining the antenna size and


Fig. 2. Metallic items of various shapes and sizes that are typically encountered in RFID applications.

structural complexity at an acceptable level.

Nonetheless, as illustrated in Fig. 2, conductive items of various shapes and sizes are encountered through the whole spectrum of RFID applications. Examples include industrial asset management, machine inventory at construction sites, tracking of containers, vehicles and train cars through a transportation chain, monitoring of elevators and escalators, and item level identification of small metallic items, such hardware tools, kitchen ware, tin cans and spray bottles. Thus, the need for tag antennas performing well in the proximity of conductive bodies is eminent. Correspondingly, a great amount of research on such antennas has been conducted while the interest in the topic remains high. Finally, the general design flow of antennas for metal mountable tags is illustrated in Fig. 3.

This article reviews the progress made in the field, discusses the various types of antennas and design approaches used in the metal mountable tags and presents future prospects. The rest of the text is organized as follows. Section II introduces the concept of tag read range which will be used as tag performance metrics throughout the paper, Sections III and IV discuss metal mountable tags based on antennas with and without ground planes, respectively. Discussion and future prospects are provided in Section V.

## II. Read Range as Tag Performance Metrics

The maximum distance at which a tag can be detected by the reader is an important practical tag performance indicator, which is readily understood not only by the antenna engineers, but also by people with other areas of expertise. Using the read range to evaluate the performance of RFID tags has also the advantage that it can be measured wirelessly, using rather unsophisticated equipment. This way, the problematic invasive small antenna measurements are avoided and separate characterization of the tag IC is not required.

### A. *Measuring and Simulating the Read Range*

Normally, the read range of passive tags is limited by the forward link operation, i.e. the efficiency of the wireless power transfer from the reader to the tag IC. Assuming free-space conditions for site-independent comparison, the obtainable tag read range at the spatial observation angles $\varphi$ and $\theta$ of a spherical coordinate system centered at the tag is given by [71]

$$d_{tag}(\phi,\theta)=\frac{\lambda}{4\pi}\sqrt{\frac{\chi_{tag}(\phi,\theta),\tau e_{r,tag}D_{tag}(\phi,\theta)EIRP}{P_{ic0}}}; \quad (1a)$$

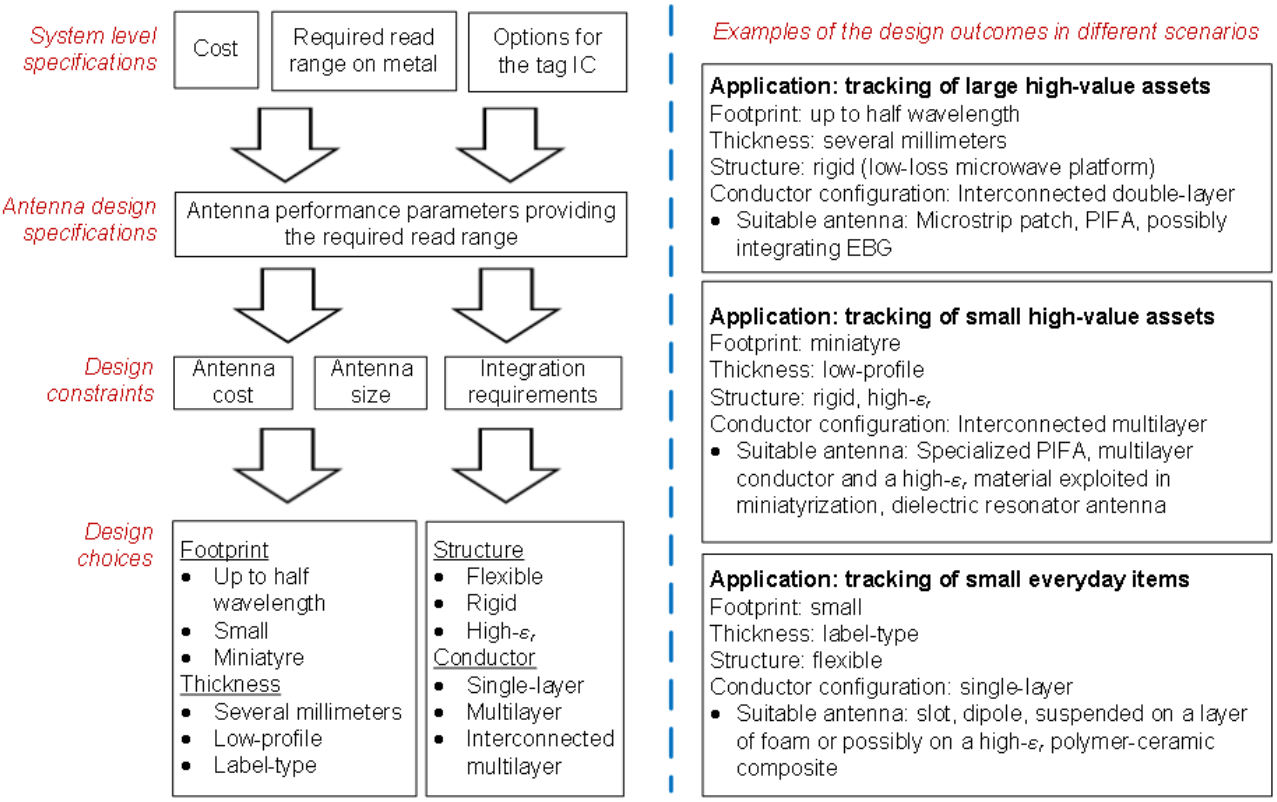


Fig. 3. Design flow of metal mountable tags exemplified.

$$\tau = \frac{4\,\mathrm{Re}(Z_{tag})\mathrm{Re}(Z_{ic})}{\left|Z_{tag}+Z_{ic}\right|^2}, \qquad (1b)$$

$$d_{tag}(\phi,\theta) = r\sqrt{\frac{\chi_{tag}EIRP}{G_{r,tx}P_{th}}}, \qquad (2)$$

where $\lambda$ is the wavelength of the carrier tone emitted by the reader, *EIRP* is the regulated equivalent isotropic radiated power, $P_{ic0}$ is the wake-up power of the tag IC, $\chi_{tag}$ is the mutual polarization power efficiency between the tag and reader antennas, $e_{r,tag}$ is the tag antenna radiation efficiency, $D_{tag}$ is the tag antenna directivity, and $\tau$ is the antenna-IC power transfer efficiency determined by the antenna and IC impedances $Z_{tag}$ and $Z_{ic}$, respectively. Equation (1a) is a direct implication of Friis' simple transmission equation.

While equation (1) shows explicitly how the tag antenna properties and impedance matching with the tag IC affect the read range, all the required data may not always be available for the computation. However, based on the wireless measurements performed in an anechoic chamber on fully assembled tags, a different equation is obtained from the Friis' simple transmission equation and (1). In this measurement, the transmit power of the reader is ramped down during the interrogation of the tag under test and the lowest transmit power (threshold power; $P_{th}$) at which the tag remains responsive, is recorded. Most commonly, the threshold power is defined with respect to the *query* command to which the tag replies with its identification code. The obtainable tag read range is given by [17]

where $r$ is the separation of the polarization-matched reader and tag antennas, $G_{r,tx}$ is the realized gain of the reader antenna including the combined cable and impedance mismatch losses. Here, the observation direction $(\varphi,\theta)$ is determined by the orientation of the tag under test with respect to the transmit antenna.

Normally, $d_{tag}$ is reported assuming $\chi_{tag}$=1, while sometimes $\chi_{tag}$=1/2 is imposed to estimate the polarization loss between the predominantly linearly polarized tag antennas and circularly polarized reader antennas. If the observation angles are not specified, it is assumed that the read range value is the maximum value over all the spatial angles. To summarize the above discussion: $d_{tag}$ given in equations (1) and (2) is the forward link limited tag read range obtainable in free-space conditions with an EIRP-compliant transmitted power when the maximum reader antenna gain is pointed toward the tag.

Henceforth, all the tag read range values quoted in this article will be scaled to correspond with *EIRP* = 4 W (regulated EIRP e.g. in the U.S.), $P_{ic0}$ = –18 dBm and $\chi_{tag}$ = 1. This allows for the fair comparison of the results reported by authors using different measurement configurations, tag ICs with different wake-up powers, as well as various EIRP regulations. It should be noted here that over the years, especially the tag IC wake-up powers have improved much and as seen from equation (1) this parameter plays a major role

in the tag read range. For clarity the asterisk notation: $d_{tag}$* is used to distinguish the scaled read range values from those reported in the cited articles.

In addition to read range, we have considered the operable bandwidth as a qualitative tag performance indicator. Currently, the global UHF RFID frequency range of 840-960 MHz is divided into regionally regulated sub-bands which are centered approximately at the frequencies of 866 MHz (lower), 915 MHz (middle) and 953 MHz (upper). Single band (S) tags are specifically designed for one of these ranges. Broadband (B) tags achieve broader bandwidths of several tens of megahertz. Wideband (W) tags are operable with similar performance on at least two of the lower, middle, and upper ranges of the of 840-960 MHz band.

### B. *Read Range of Dipole Type Tags on Metal*

Dipole type tag antennas are presently popular in UHF RFID. They have simple single-layer structure fit for label type tags. Moreover, the dipole antenna radiation pattern is omnidirectional in the plane perpendicular to the dipole axis. Compared with directive antennas, this provides broader spatial coverage for power harvesting. Size-reduction techniques for dipole type antennas are also well-established [29][30][31]. Dipole type tag antennas can also provide sufficient platform-tolerance to guarantee the reliable identification of most dielectric objects with low permittivity ($1 \le \varepsilon_r \le 5$) [18][19][32][33][34][35].

The influence of a conductive surface on a dipole antenna is, however, a more severe performance issue. To exemplify the influence of this phenomenon on the properties of dipole type antennas, we have conducted a simulative study on a straight quarter-wave dipole and a T-matched folded dipole (a popular tag antenna structure) placed parallel to conductive surface. The simulations were conducted with ANSYS HFSS version 13. The studied antennas are shown in Fig. 4.

The quarter-wave dipole was simulated at the distance of 1.5 mm from a metal plate (conductivity: 58 MS/m) with the

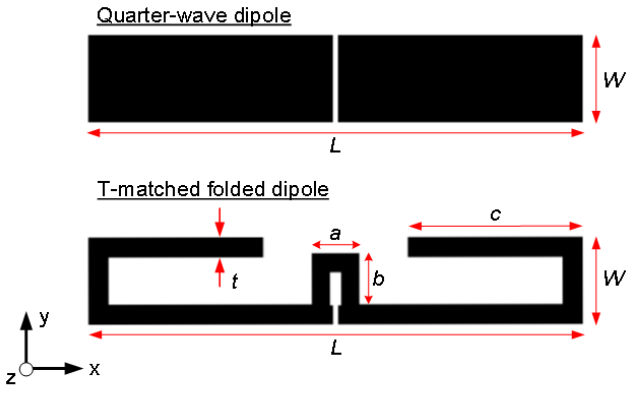


Geometrical parameters in millimeters

| *L* | *W* | *t* | *a* | *b* | *c* |
|---|---|---|---|---|---|
| 86.6 | 15 | 3 | 8 | 9.1 | 30.3 |

Figure 4. Studied dipole antennas.

size of $140 \times 50 \times 5$ mm$^3$. The simulated antenna was not matched to specific tag IC impedance, but we chose the 50-Ω feed port power in the simulation tool so that the amount of power transferred to the antenna structure is 100 mW. Figure 5a presents the surface current density on the antenna and metal plate beneath it. The arrows show a snapshot of the current flow at a fixed time instant. From this illustration, it is seen that the surface current densities on the antenna and metal surface beneath it are of the same order of magnitude, but the current flow directions are opposite.

The resulting effect on the conventional antenna parameters is summarized in Fig. 6a. At small separations from the metal, the antenna is almost short-circuited. This leads to very low values of the radiation efficiency. As the antenna-metal separation is increased up to 3 mm, which is still feasible in some RFID applications, the radiation efficiency is increased to 25%. However, the antenna resistance still remains low making the impedance matching problematic.

The study on the T-matched folded dipole demonstrates further the impact of the metal proximity on the properties of a common class of tag antennas. In general, tag antennas need to be conjugate-matched with capacitive tag ICs. For short dipoles, T-matching technique can be used to transform the capacitive antenna impedance to inductive [16]. In practice, this is realized by forming a short circuit current path parallel to the antenna terminals (params. *a* and *b* in Fig. 4).

Since the footprint size of tag antennas is a major concern, the dipole arms are typically folded to lower the fundamental antenna resonance within the same footprint. Following these two widely employed design approaches, we chose the parameters *a*, *b*, and *c* in Fig. 4 to achieve antenna impedance close to $15+j150$ Ω (at 866.6 MHz) at the distance of 1.5 mm from the metal plate. This serves as an example of a typical target value in a practical tag design scenario. Since the aim of the study is to exemplify the general features of dipole tags near metal, a specific antenna substrate material was not considered, but the simulations were conducted in air. The features arising from the metal proximity are, however, shared by dipole tags on low-permittivity platforms, including circuit boards, plastics, and foams.

To achieve a fair comparison with the quarter-wave dipole, we adapted the 50-Ω feed port power in the simulation so that 100 mW was delivered to the antenna. As seen from Fig. 5b, the surface currents on the antenna and metal plate are of the same order of magnitude, but flow in the opposite directions. Thus, this antenna shares the same ailments with the quarter wave dipole when it is placed parallel to a conductive surface. The simulated tag performance parameters are summarized in Fig. 6b. The T-matched folded dipole exhibits its self-resonance frequency within the studied frequency range. Below the resonance frequency, the antenna impedance is inductive providing conjugate matching to the tag IC. In this case the antenna-IC power transfer efficiency ($\tau$) is maximized near 866.6 MHz ($\tau \approx 1$). However, the radiation efficiency remains low, below 5%, up to the antenna-metal separation of

3 mm. At the separation of 1.5 mm, the radiation efficiency is only 2%, but the tag still achieves a seemingly high read range of approximately 3 meters at the matched frequency of 866.6 MHz. This is because the proximity of the metal surface increased the antenna directivity to approximately 4.3 dBi (Fig. 6b), which is notably higher than the value for a dipole in free-space.

As a summary, T-matched folded dipole tag in metal proximity suffers from low efficiency with resistance sharply decaying toward zero at frequencies away from the antenna self-resonance frequency. This results in limited read range and narrow-band matching. Moreover, the simulated antenna parameters are sensitive toward the antenna-metal separation. Therefore, in practical scenarios with the antenna-metal separation varying from object to object, the tag read range is likely less than the simulated peak value.

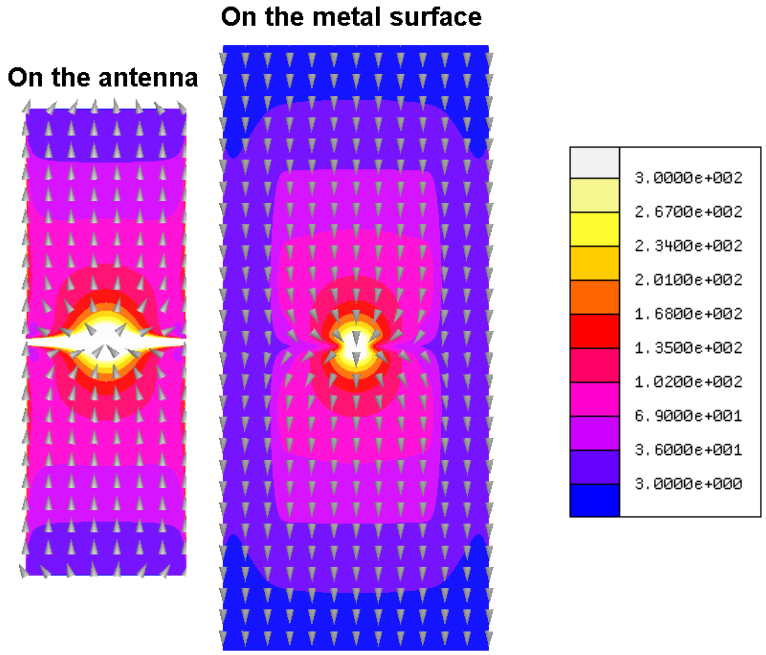


Figure 5a. Surface current density [A/m] on the quarter-wave dipole and metal plate beneath it (separation: 1.5 mm) at 866.6 MHz. The antenna is accepting 100 mW.

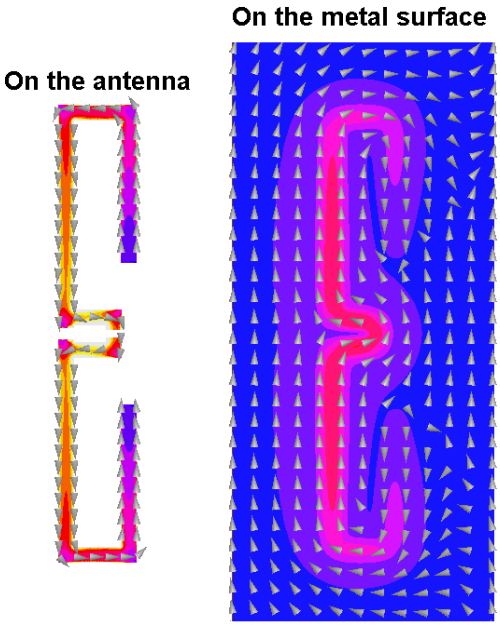


Figure 5b. Surface current density [A/m] on the T-matched folded dipole and the metal plate beneath it (separation: 1.5 mm) at 866.6 MHz. The antenna is accepting 100 mW.

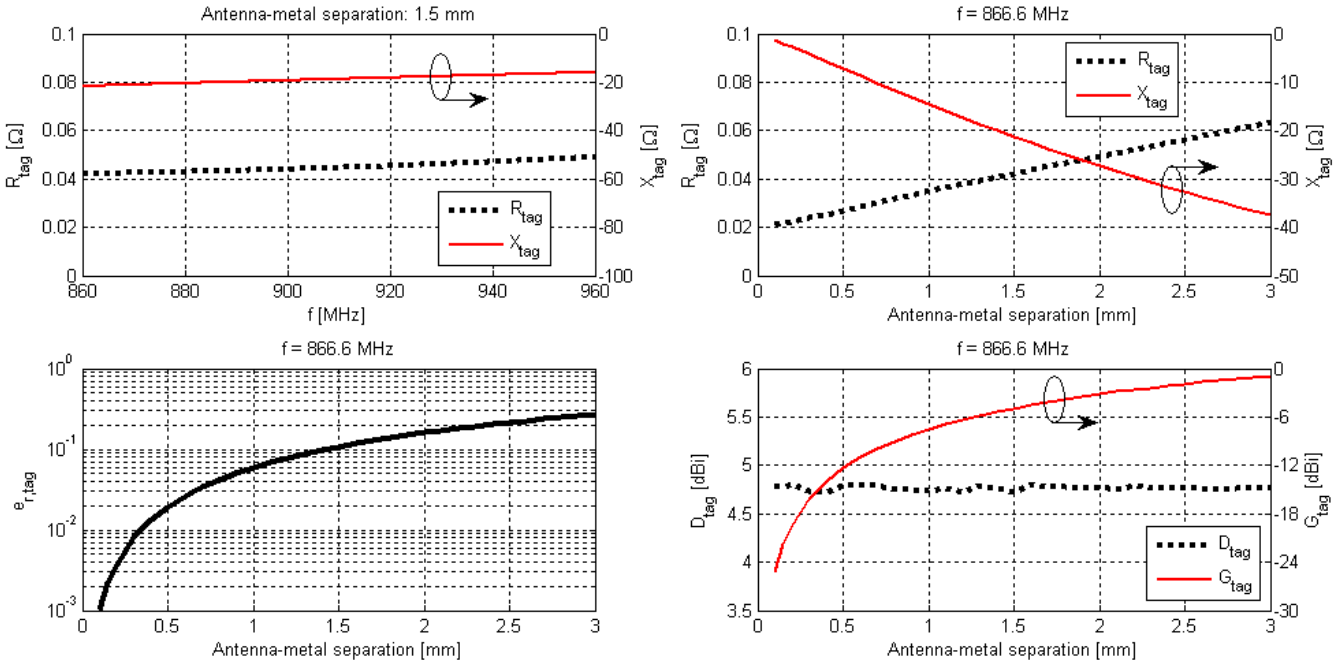


Figure 6a. Properties of the quarter-wave dipole placed parallel to a metal plate. Radiation properties are reported in the direction of the positive z axis in Fig. 4.

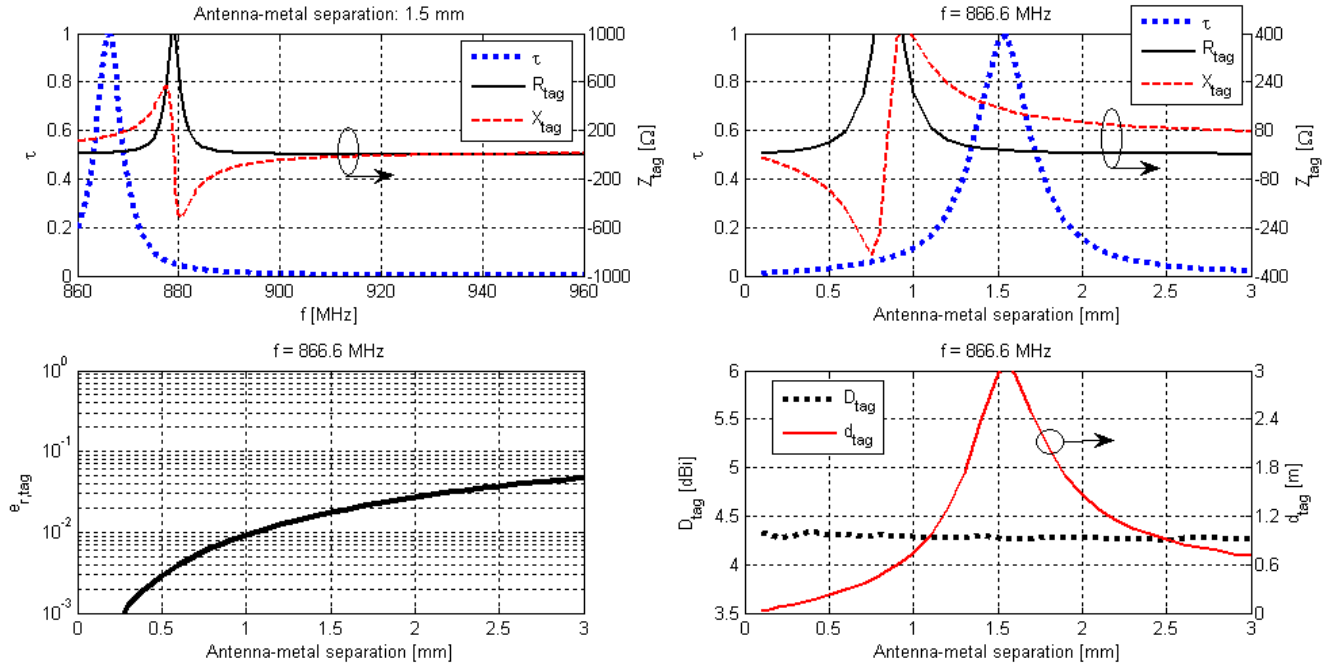


Figure 6b. Properties of the folded T-matched dipole placed parallel to a metal plate. Radiation properties are reported in the direction of the positive z axis in Fig. 4.

## III. Antennas with Ground Plane

Microstrip patch antennas have been widely used in the wireless devices, where low-profile planar antennas with moderate gain are needed [14]. Later, the planar inverted-F antennas (PIFA) with similar radiation characteristics, but even smaller footprints and favorable multi-resonant features became popular cell-phone antennas [36][37]. The ground plane included in these antennas also helps to electromagnetically isolate them from the matter behind the ground plane. Thanks to this feature, these antenna types were the first ones to be used in metal mountable tags. Until today, an abundance of modifications to the canonical patch antennas and PIFAs have been proposed to achieve size-reduction, bandwidth improvement, and longer tag read ranges. Later, the electromagnetic band gap (EBG) structures [38] enabled the development of metal mountable tags based on dipole antennas integrating EBG structures. All these developments are reviewed and summarized in the following subsections.

### A. *Microstrip Patch Antennas*

The conventional microstrip patch antenna is composed of a conductor patch patterned on a dielectric substrate material on top of a larger conductor area acting as the ground plane. In the transmitting mode, the antenna is driven by a time-varying potential difference between the patch and ground. This sets up a time-varying electric between the two conductors and at certain frequency bands the related electromagnetic energy leaves the structure efficiently as radiation. Since tag ICs have differential inputs, patch-type tag antennas need to be equipped with a balanced self-matching structure. The operable frequency range of the antenna is determined predominantly by the size of the patch and the dielectric constant of the substrate material. Normally, the viable substrate thicknesses are found in the range of $0.01\lambda$-$0.05\lambda$. This enables fairly low-profile antenna structures. [14]

At high frequencies, the current flows predominantly in a thin layer at the surface of good conductors. This is known as the skin effect. Thus, in the ground plane of patch antennas, the current flows mostly near the surface facing the dielectric material, so that there is little interaction with the current in the ground plane and the materials behind it. For this reason, patch antennas are considered advantageous for metal mountable tags. By making the ground plane larger than the patch, the antenna-metal interaction through the fringing fields at the patch edges can be further suppressed. However, this comes with the cost of increasing the tag size.

In one of the earliest studies on antennas for metal mountable tags, a rectangular patch antenna patterned on copper-clad RT/Duroid TMMi10 high-frequency laminate ($\varepsilon_r$=9.8, tan$\delta$=0.002) was investigated [39]. The size of the antenna ground plane is $100\times100$ mm$^2$ and the laminate thickness is 3.2 mm. An identical layer of the material was placed also on the opposite side of the ground plane to separate it further from the metal surface backing the tag. Full-wave EM simulations with $18\times20$ cm$^2$ metal plate backing the antenna showed that a rather high gain of 5 dBi was obtainable. Given that good impedance matching to a tag IC was arranged, this corresponds to read range $d_{tag}$* = 23 m. Although the studied antenna may be too large for most applications, the presented results clearly demonstrated the impressive read ranges achievable with patch antennas.

Recently, a holistic simulation-based design of a rectangular patch antenna (Fig. 7) patterned on copper-clad RT/Duroid 5880 high-frequency laminate ($\varepsilon_r$=2.2, tan$\delta$=0.0009) was presented [40]. The tag is intended for tracking of large and high-value conductive items. In this application, high tag read on conductive surfaces is paramount while the tag size is not as strictly limited. To guarantee the maximal tag performance on metal, a $20\times20$ cm$^2$ copper plate backing the antenna was included in all the simulations for design optimization. In this process, a clearance of 16 mm between the patch and substrate

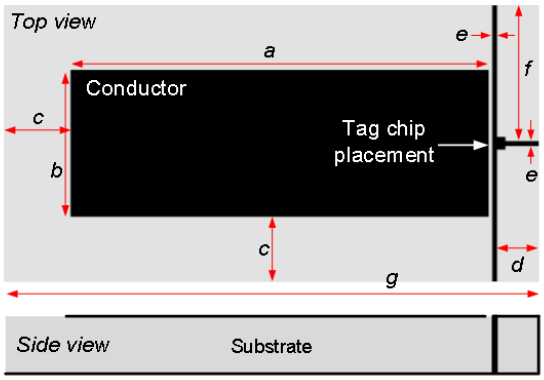


Geometrical parameters in millimeters

| *a* | *b* | *c* | *d* | *e* | *f* | *g* |
|---|---|---|---|---|---|---|
| 102.75 | 36 | 16 | 10.5 | 1 | 33.5 | 131.25 |

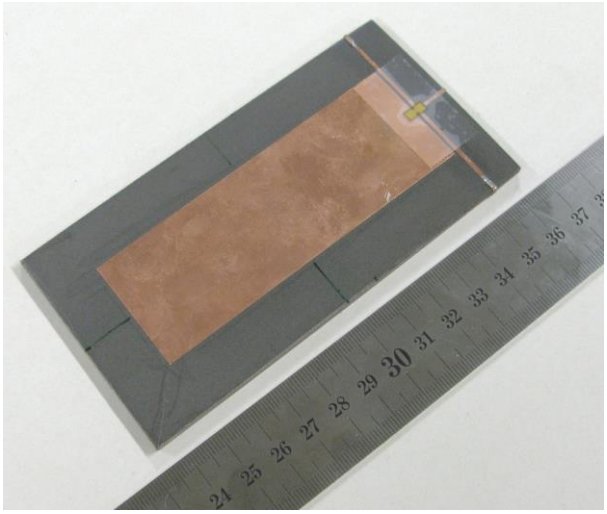

Figure 7. Patch antenna studied in [40].

edges (param. *c* in Fig. 7) was found to suppress the antenna-metal interaction through the fringing fields at the patch edges sufficiently to provide the high radiation efficiency of 89%. Directive radiation pattern and suitable impedance pre-matching were achieved by adjusting the patch size (params. *a* and *b* in Fig. 7). To fully conjugate match the antenna with capacitive tag ICs, the chip was placed at the patch edge so that one of the chip terminals is connected to the patch and the other is joined with the ground through narrow inductive strips wrapping over three of the substrate edges. The antenna impedance was then controlled by the dimensions (params. *e* and *d* in Fig. 7) of this inductive matching network. The overall size of the studied tag is $131\times68\times3.3$ mm$^3$ and it achieved the high read range $d_{tag}$* = 25 m.

The trapezoid patch [41] has an approximately equal footprint size ($110\times80$ mm$^2$) compared with the tag presented in [40]. The overall thickness of the tag, however, is only 0.8 mm. In this antenna, the impedance matching was realized by adjusting the height and length of one of sides of the trapezoid patch. The tag IC was placed immediately at the patch edge and shorted to ground through a via. The studied tag achieved the read range $d_{tag}$* = 10.7 m. While the antenna topologies [40] and [41] are in essence the same (solid patches with approximately equal sizes connected to ground through the tag IC), the performance comparison between the two accentuates the principal design trade-off shared by virtually all antennas for metal mountable tags: thickness vs. performance.

In many applications, even smaller tags are needed. For instance, a rectangular patch on a double-layer RF-4-foam substrate achieved the overall size of only $50\times47.5\times3$ mm$^3$ [42]. The antenna is composed of two rectangular patches shorted to the ground through narrow strips at one corner of each patch to form two symmetrical radiating elements. The authors found this to be a favorable approach to reduce the antenna-metal interaction compared with a single radiating patch. The tag IC was mounted in a loop which proximity couples to the two radiating patches and provides impedance matching. The studied tag achieved the read range $d_{tag}$* = 8.7 m.

On the other hand, also various other design approaches for size-reduction and bandwidth improvement have been studied. One of the successfully applied techniques is the slot loading. With this method, the path of the radiating current can be increased with cut-outs in the patch. This lowers the antenna self-resonance frequency and thereby provides the means for antenna miniaturization, given that excessive current cancellation is avoided [30]. Moreover, the antenna impedance can be tuned by placing the cut-outs in regions away from the main current path. One of the earliest demonstrations of this design approach in metal mountable tags is an L-shaped slot in a conductor patch on double-layer FR4-foam substrate [43][44]. A favorable feature in this design is the non-monotonic reactance frequency-response at the frequencies of interest. This helps to achieve broadband matching. The developed tag has the overall size of $90.5\times54.5\times5$ mm$^3$ and it

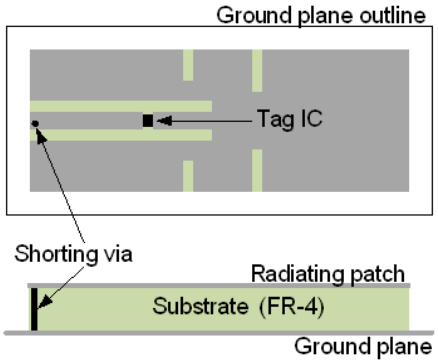


Figure 8. Patch antenna studied in [45].

achieved the read range $d_{tag}$* = 13 m.

Later, for instance, a rectangular patch antenna shown in Fig. 8 with a pair slots extending from the patch edges towards the center has been studied [45]. Compared with the tag antenna presented in [43][44], this design is thinner and smaller, but also exhibits a non-monotonic reactance frequency-response favorable for impedance matching. The overall size of the studied tag is $80\times40\times1.6$ mm$^3$ and it achieved the read range $d_{tag}$* = 7.4 m.

A similar design, where strategically placed U-shaped slots near the patch edges provided improved bandwidth through an appropriate reactive loading of the antenna impedance, was reported in [46]. The overall size of this tag is $96\times50\times2$ mm$^3$ and it achieved the read range $d_{tag}$* = 7.6 | 8.8 m in European | U.S. RFID frequencies. Another design [47] with very similar tag size of $98\times50\times1.6$ mm$^3$ includes a T-shaped insertion formed inside a rectangular slot for reactive loading. The tag achieved the read range $d_{tag}$* = 8.5 | 8.7 m in European | U.S. RFID frequencies.

More recently, a dual-patch antenna loaded with several slots was studied [48]. The antenna structure is shown in Fig. 9. In this design, the inductive feed loop provided an adequate pre-matching for most tag ICs, while the additional parametric study provided by the authors shows how to adapt the shape of the slot configuration (reactive loading) to fully impedance-match the antenna to given tag IC. The antenna was patterned on copper-clad RT/Duroid 5870 high-frequency laminate ($\varepsilon_r$=2.3, tan$\delta$=0.0012). The overall size of the tag is only $50\times50\times1.6$ mm$^3$ and it achieved the read range $d_{tag}$* = 5 m. Compared with a similar antenna [42] with solid rectangular

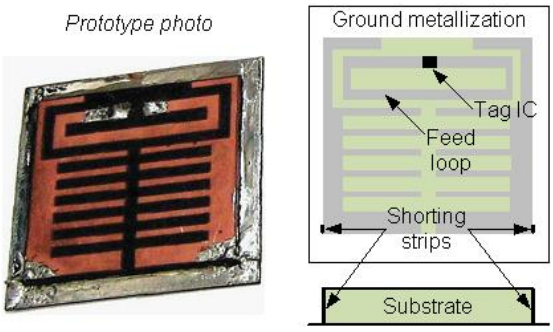


Figure 9. Patch antenna studied in [48].

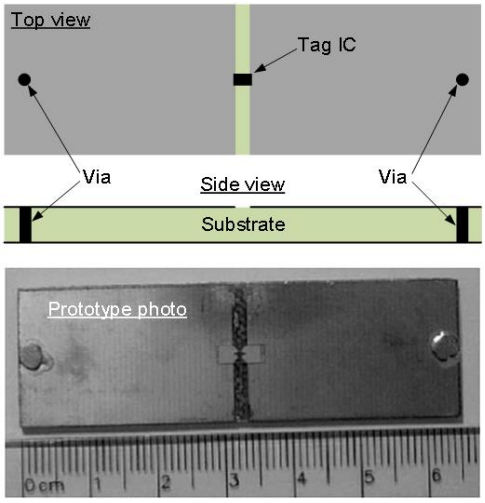


Figure 10. Patch antenna studied in [49].

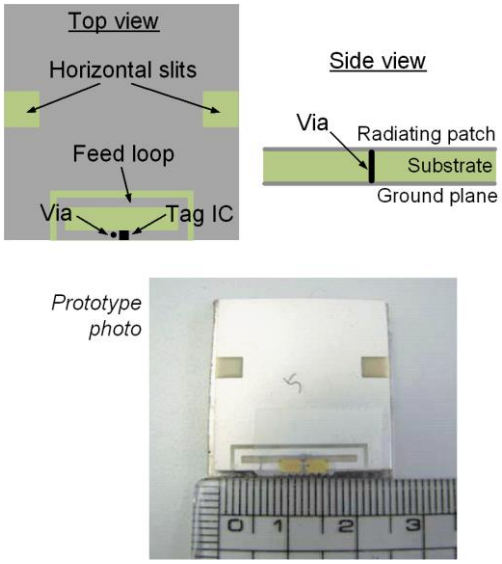


Figure 11. Patch antenna studied in [55].

patches on a double-layer FR4-foam substrate, the multi-slotted version provided considerably thinner and simpler structure.

Shorting the patch to the ground at one or more strategic locations is another design approach which has been found useful in the development of patch antennas for small metal mountable tags. The antenna shown in Fig. 10 makes use of this approach by adapting the structure of a high-impedance unit cell as a radiator [49]. The overall size of the tag is $65\times20\times1.5$ mm$^3$ and it achieved the read range $d_{tag}$* = 6.9 m. In addition to the slim structure, a distinctive feature in this design is the oblong shape, which in some applications may be a good alternative to the commonly more square-shaped patch tags. A further study [50] showed how to reduce the antenna footprint by inserting a non-connected intermediate conductor layer in between the patch and the ground. However, this increased the thickness and structural complexity. Additionally, a more performance oriented adaption of the same structure was analyzed in [51] with the note on reduction of the mutual capacitance between the two patches by sloping of the patch edges facing each other. This made the antenna more inductive which was favorable for impedance-matching the antenna to capacitive tag ICs.

Multiple proximity coupled grounded patches can provide bandwidth improvement. For instance, designs with one or two parasitic patches loading the driven patch were studied in [52]. The patch sizes were chosen to have slightly different lengths, so that the antenna is excited with multiple modes. With the appropriate separation between the patches, the antenna achieved a fluctuating reactance frequency-response favorable for wideband impedance matching. The configuration with two parasitic patches provided broader bandwidth, but had a larger footprint. The overall tag size with one parasitic patch is $85\times58\times1.6$ mm$^3$ and with two parasitic patches $85.5\times83\times1.6$ mm$^3$. The designs achieved the read ranges $d_{tag}$* = 11 | 4.8 m and $d_{tag}$* = 11.4 | 7.1 m in the European | U.S. RFID frequencies.

A similar design with the tag IC mounted in a loop, which proximity coupled to four parasitic patches was studied in [53]. The parasitic patches had different sizes and each of them included a via to ground. The overall size of the tag is $80\times80\times2$ mm$^3$ and it achieved the read range $d_{tag}$* = 8 m at 915 MHz. The simulation results suggested that similar read range could be obtained throughout the global UHF RFID frequency range. However, the polarization properties of the antenna vary with frequency, depending on which parasitic patch is active at the specific sub-band.

The authors of [54] studied a patch tag with a new kind of proximity-coupled feed structure. The radiating patch and the ground plane were formed by bending a thin aluminum sheet into U-shaped cross-sectional view around low-permittivity and low-loss polystyrene foam. A straight conductive trace was immersed in the foam at an equal distance from both the patch and ground. The trace was shorted from both ends to the ground and the tag IC was placed near one of the shorting pins. The antenna exhibited a non-monotonic reactance frequency-response which enabled broadband operation. The tag achieves the read range $d_{tag}$*=14.1 m with the overall tag size of $72.1\times25.5\times3.2$ mm$^3$.

By recalling that the cavity resonator model (electric field oscillating in between the patch and the ground within the substrate material) is a widely used approximate analytical model for a patch antenna, it is understood that the size-reduction may be achieved by using a high-dielectric substrate material. This makes the structure appear electrically large compared with its actual physical dimensions and thereby lowers the frequency of the fundamental resonance mode. By combining this size-reduction technique with slot-loading and a proximity-coupled loop feed, the authors of [55] proposed a miniaturized patch tag (Fig. 11) on a ceramic substrate with the relative permittivity of 48. In this antenna, the feed loop was connected to ground through a via. The tag has the overall size of only $25\times25\times3$ mm$^3$ and it achieved the read range

Table 1. Comparison of metal mountable patch tags.

| Ref. | [40] | [41] | [45] | [46] | [48] | [49] | [50] | [52] | [54] | [55] |
|---|---|---|---|---|---|---|---|---|---|---|
| Tag size [mm$^3$] | $131\times68\times3.2$ | $110\times80\times0.8$ | $80\times40\times1.6$ | $96\times50\times2$ | $50\times50\times1.6$ | $65\times20\times1.5$ | $32\times18\times3.2$ | $85.5\times83\times1.6$ | $72.1\times25.5\times3.2$ | $25\times25\times3$ |
| *ka* | 1.40 | 1.28 | 0.84 | 1.02 | 0.67 | 0.64 | 0.35 | 1.12 | 0.72 | 0.33 |
| Metal plate [cm$^2$] | $20\times20$ | $40\times40$ | $30\times30$ | $30\times30$ | $17\times17$ | $17\times17$ | $17\times17$ | $40\times40$ | $20\times20$ | $20\times20$ |
| $d_{tag}$* [m] | 25 | 10.7 | 7.4 | 7.6 | 5 | 6.9 | 3.3 | 7.1 | 14.1 | 10.1 |
| Bandwidth | S | S | B | W | B | S | S | W | B | S |

S = single-band, B = broadband, W = wideband

$d_{tag}$* [m] is the reported tag read range referred to $P_{ic0}$ = −18 dBm and EIRP = 4 W under perfect polarization alignment.

$d_{tag}$*=10.1 m. As discussed in Section III.C, high-permittivity ceramic and polymer-ceramic composite substrates have been successfully applied also in the development of tag antennas without ground plane for the on-metal application.

Finally, Table 1 summarizes the performance of different metal mountable tags based on microstrip patch antennas.

### B. *Planar Inverted-F Antennas*

A planar inverted-F antenna (PIFA) is a microstrip loaded with a short circuit. In its standard single-band configuration, PIFA is a patch shorted to ground from one location (single via or a shorting wall at one of the radiating edges) and driven by a time-varying potential difference between the patch and ground antenna at another location. In this configuration, the resonant length of the patch element is approximately quarter wavelength and the cross-sectional view of the conductor structure excluding the ground plane resembles the letter F [14][37]. However, as seen below, some PIFAs in this section incorporate structural modification beyond the standard configuration explained above. Also, some of the patch tags discussed in Section III.A may fit under the above definition of a PIFA. Nonetheless, we have followed the original authors' classification of the antenna types based on the design approaches they have employed.

As grounded structures, PIFAs benefit from the built-in antenna-conductor isolation when they are mounted on conductive surfaces. In performance critical applications, this feature could be further enhanced by inserting an additional layer of dielectric material beneath the antenna ground plane. This approach was studied in [56]. Although the improvement comes with the price of increased antenna thickness, high read range $d_{tag}$*=22.3 | 15.6 m was achieved with the overall tag size $100\times80\times6.5$ | 3.2 mm$^3$. This demonstrates again the fundamental thickness-performance trade-off shared by virtually all metal mountable tags. A more size-oriented PIFA design for tags mountable on conductive items was proposed in another early study [57]. This antenna is a square patch shorted at one corner to the ground through the tag IC while the opposite corner is shorted to the ground through a shorting wall. The tag has the overall size of $59\times59\times3$ mm$^3$ and it achieved the read range $d_{tag}$*=8.9 m.

Shortly afterwards, a PIFA with a low-permittivity foam substrate was reported [58]. By folding the main radiator into an intermediate layer, the antenna was made to appear electrically larger. Mounting the tag IC over U-shaped slot patterned in the top face of the main radiator provided the means for impedance matching by varying the slot dimensions. The tag has the overall size of $50\times60\times4$ mm$^3$ with the measured read range $d_{tag}$=4 m. Although the necessary information for computing the scaled read range is not provided, equipping the tag with a present-day tag IC is expected to improve the read range further. Compared with [56], the discussed antenna provided a more compact size and instead of specialized microwave antenna substrates used in [56][57], it was based on a low-cost and flexible foam substrate.

While the above-discussed PIFAs are operable at a specific sub-band of the global RFID frequency range, the authors of [59] showed that dual-band operation was attainable within the same antenna footprint. The studied antenna shown in Fig. 12 is composed of a rectangular patch connected from one of non-

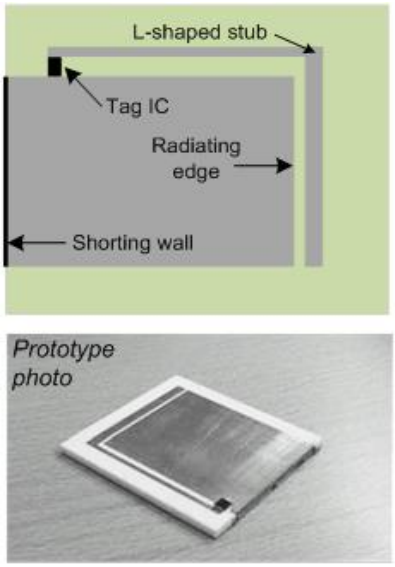


Figure 12. PIFA studied in [59].

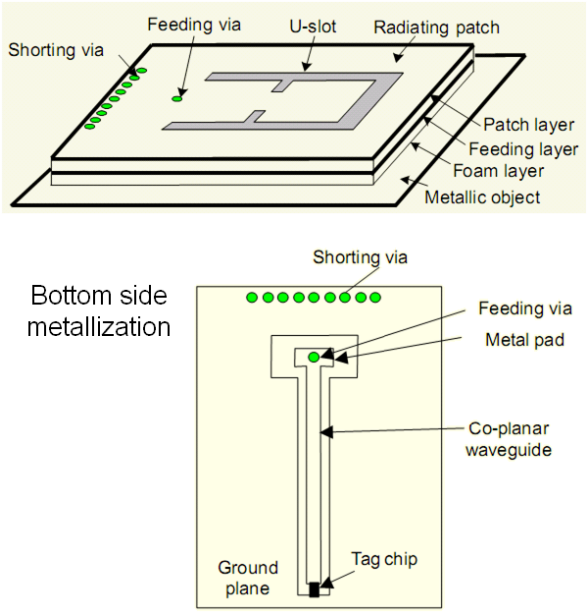


Figure 13. PIFA studied in [60].

radiating edges to an open-ended L-shaped stub and from one of the radiating edges to the ground through a shorting wall. The tag IC was mounted over a gap between the patch edge and the open-ended L-stub, which acted as the second ground connection of the conventional PIFA. Importantly, the authors found that the structure provided dual-band matching with a tag IC. Moreover, they showed that the capacitance between the stub and the radiating patch edge can be used to adjust the frequency separation between the two matched frequencies. The tag has the overall size of $59\times59\times3$ mm$^3$ and it achieved the read range $d_{tag}$*=8.9 m in the European RFID band. Simulations suggested that the read range $d_{tag}$*=9.8 m would be attained at the upper matched frequency of 940 MHz. Moreover, by adjusting the gap between the radiating edge of the patch and the stub, the authors also managed to bring the simulated upper matched frequency down to 915 MHz with $d_{tag}$*=9.3 m.

At the same time, further size-reduction on single-band PIFAs was reported in [60]. The studied antenna, shown in Fig. 13, consists of a U-shaped radiating slot in the top layer of a square-shaped circuit board and an impedance tuning structure patterned in the bottom layer. A via joins the top layer metallization to a rectangular pad, which terminates a co-planar waveguide patterned in the bottom layer metallization. The other end of co-planar waveguide is terminated with the tag IC. The top and bottom metallization were joined through several vias located at an edge of the board. Finally, a 1-mm foam layer was attached to the bottom layer to separate the whole structure from the metal surface. While the exact shape of the U-slot and the board size predetermined the antenna properties, according to the authors, the size of the rectangular pad in the bottom layer played a key-role in the impedance tuning. The tag has the overall size of $46\times46\times3.4$ mm$^3$ and it achieved the read range of $d_{tag}$= 4.5 m. Although the necessary

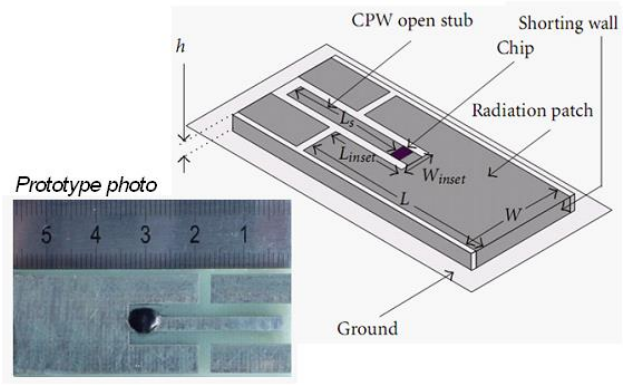


Figure 14. PIFA studied in [61].

information for computing the scaled read range is not provided, equipping the tag with a present-day tag IC is expected to improve the read range further.

More recently, another small PIFA, shown in Fig. 14, utilizing the co-planar waveguide as the impedance matching structure was studied [61]. Compared with [60], this antenna has even smaller footprint and simpler structure, where both the impedance matching structure and the main radiator are located in the top layer. In this way an additional foam layer is not needed. Moreover, the co-planar waveguide stub is open-ended. A shorting wall connects one edge of the top metallization to the bottom layer acting as the ground. The radiation originates predominantly from the patch in the top layer, which is the co-planar metallization around the middle trace of the open-ended waveguide. According to the authors, one of the advantages of the structure is that by changing the stub length, the low-resistance and inductive antenna impedance changes monotonically over a sufficient range to tune the design for most tag ICs. Thus, the antenna impedance matching is conveniently controlled with a single parameter. The tag has the overall size of $56\times22\times3$ mm$^3$ and it achieved the read range $d_{tag}$* = 11.8 m.

Finally, Table 2 summarizes the performance of different

Table 2. Comparison of metal mountable PIFA tags.

| Ref. | [58] | [59] | [60] | [61] |
|---|---|---|---|---|
| Tag size [mm$^3$] | $50\times60\times4$ | $62\times51.3\times3$ | $46\times46\times3.4$ | $56\times22\times3$ |
| $ka$ | 0.74 | 0.76 | 0.61 | 0.57 |
| Metal plate [cm$^2$] | $20\times20$ | $46\times46$ | $46\times46$ | $20\times20$ |
| $d_{tag}$* [m] | > 4 | 8.9 | > 4.5 | 11.8 |
| Bandwidth | S | W | S | S |

S = single-band, B = broadband, W = wideband

$d_{tag}$* [m] is the reported tag read range referred to $P_{ic0}$ = −18 dBm and EIRP = 4 W under perfect polarization alignment.

metal mountable tags based on PIFAs.

C. *Antennas integrating EBG structures*

Electromagnetic band gap (EBG) structures are a class of metamaterials defined as structures that prevent or assist the propagation of electromagnetic waves in a certain frequency band for all incident angles and polarization states [38]. In antenna applications EBG structures can be used to form conductive surfaces with reflection phase adjustable from −180° to 180° and to suppress the excitation of surface waves. This allows for the development of low-profile antennas (reflection phase) and improving the efficiency of antenna with ground planes (surface wave suppression). As discussed below, both these features have been found useful in the development of antennas for metal mountable tags.

Article [62] presented a performance comparison of microstrip patch antennas with regular and EBG ground planes mounted on metal plates of different sizes. The studied antennas had otherwise the same structure as those studied earlier in [39], but the second layer of the high-frequency laminate beneath the patch ground plane was removed. The EBG structure was based on circular slots arranged in a square lattice in the ground plane. The simulation results showed that on $50\times50$ cm$^2$ metal plate the EBG patch achieved the radiation efficiency of 94% and directivity of 5.2 dBi, while the corresponding values for the regular patch were 72% and 3 dBi. Given that good impedance matching to a tag IC was obtained, this corresponds to read range $d_{tag}$*=15.7 | 23 m for the regular | EBG patch with the overall size of $100\times100\times3.2$ mm$^3$. Moreover, the resonance frequency of the EBG patch is the same in air and on $20\times20$ cm$^2$ and $50\times50$ cm$^2$ metal plates. Both improvements; the better read range and platform-tolerance, are due to the suppressed surface waves in the EBG design.

An alternative approach exploited the in-phase reflection achievable from an EBG surface [63]. This enabled the efficient operation of a dipole antenna placed on a 2-mm layer of foam ($\varepsilon_r\approx1$) on top of the EBG structure formed by a $2\times2$ array of rectangular patches patterned on a circuit board ($\varepsilon_r$=4.5) with solid metallization in the opposite side. The structure does not contain interconnections between any of the conductor layers. This simplifies the fabrication process. The overall size of the tag is $152\times46\times3$ mm$^3$ and the authors report the measured read range $d_{tag}$=6.3 m on $80\times80$ cm$^2$ metal plate (information for computing $d_{tag}$* not provided) with virtually the same performance in air.

More recently, dipole antennas suspended on a three-layer mushroom EBG structure were studied [64]. The square-shaped mushroom caps were first patterned on both sides (S1 and S2) of a 0.2 mm FR-4 board. Then the side S2 was attached onto a non-metallized side of a 1.5 mm FR-4 board and all the mushroom caps were joined with the solid metallization on the opposite side of the 1.5 mm board through drilled vias. Finally, a 3 mm foam spacer was placed onto S1 and a folded dipole tag antenna (outer dimensions: $82\times22$ mm$^2$) was suspended on the foam. The structure of the antenna and the EBG structure are shown in Fig. 15. The authors reported the measurement results on two prototypes tags based on $5\times3$ (P1) and $4\times2$ (P2) arrays of the mushroom unit cells with the overall size of $124\times76\times4.8$ mm$^3$ and $100\times54\times4.8$ mm$^3$, respectively. Top view of the prototype P1 and the cross-sectional structure diagram are shown in Fig. 15. The reported read ranges on metal are $d_{tag}$*=12.7 m (P1) and $d_{tag}$*=7 m (P2). The performance of P2 in air was very similar, but for P1 the read range in air reduced to 9.8 m.

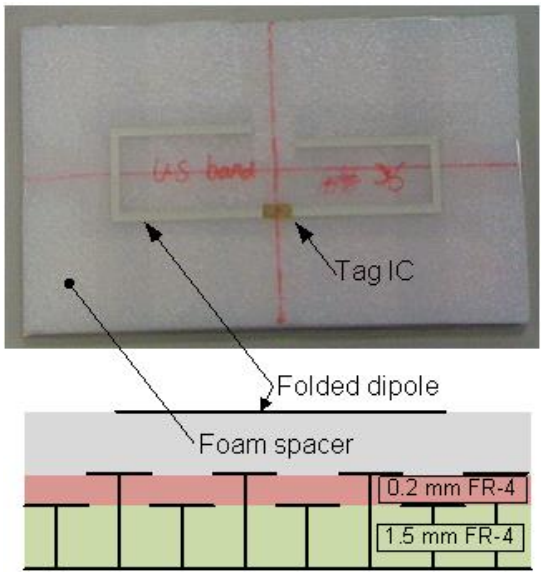


Figure 15. EBG folded dipole studied in [64].

As a summary, antennas integrating EBG structures provide an interesting approach for creating directive low-profile antennas by placing dipoles on EBG structures which provide an in-phase reflection. Including an EBG ground plane in regular patch antennas improves the antenna performance on metal through suppression of surface waves. Despite these favorable properties, it is difficult to meet the stringent size requirement of RFID tags with EBG antennas, where the size of the EBG structure dominates the overall tag size. Moreover, the desired electromagnetic properties of the EBG structures can be achieved within a limited bandwidth. As result, the

Table 3. Comparison of metal mountable EBG tags.

| Ref. | [62] | [63] | [64] | [64] |
|---|---|---|---|---|
| Tag size [mm$^3$] | $100\times100\times3.2$ | $152\times46\times3$ | $124\times76\times4.8$ | $100\times54\times4.8$ |
| *ka* | 1.33 | 1.50 | 1.37 | 1.07 |
| Metal plate [cm$^2$] | $20\times20$ | $80\times80$ | NA | NA |
| $d_{tag}$* [m] | 23 | $d_{tag}$ = 6.3 | 12.7 | 7 |
| Bandwidth | S | S | S | S |

S = single-band, B = broadband, W = wideband

$d_{tag}$* [m] is the reported tag read range referred to $P_{ic0}$ = −18 dBm and EIRP = 4 W under perfect polarization alignment.

antenna miniaturization problem turns into the problem of miniaturizing the EBG structure.

Finally, Table 3 summarizes the performance of different metal mountable tags integrating EBG.

## IV. Antennas without Ground plane

Antennas for RFID tags have very stringent requirements on size and cost. The size-reduction techniques discussed in the previous section provide antennas with compact footprints for the identification of small metallic items. However, these antennas include two or more conductor layers with interconnections and have rigid structures. Thus, in order to further reduce the manufacturing and material costs and to achieve conformal antenna structures, recently the focus of the research has been shifting toward antennas based on a single conductor layer. These developments, fuelled by the vision of label type metal mountable RFID tags, are reviewed and summarized in this section.

One of the first articles on antennas for metal mountable tags not incorporating a ground plane presented a fork-shaped antenna on an FR-4 board [65]. As seen from Fig. 16, the antenna is composed of a tapered open-ended co-planar waveguide stub loaded with two rectangular parasitic patches. The tag IC is mounted over a gap between the stub and the co-planar metallization. The distance of the parasitic patches from the stub controlled the antenna reactance while the resistance was tuned through either the length or width of the parasitic patches. The tag has the overall size of $120\times30\times3.2$ mm$^3$ and it achieved the read range $d_{tag}$* = 8.9 m on metal. The performance in free space was similar.

At the same time, the on-metal performance of a dipole suspended a foam spacer was studied [66]. The studied antenna is a combination of a T-matched dipole with spiral arms and a dipole with bent arms. These two structures are joined through vertical conductor strips on both sides of the T-matching loop to form a double T-matched dipole. According to the authors, in air the bent dipole was capacitive and the spiral-arms-dipole was inductive, but in metal proximity these roles were interchanged. In this way, the impact of metal proximity on the antenna reactance was limited and the tag was operable both in air and on metal. The tag has the overall size of $83.8\times29.9\times3$ mm$^3$ and the authors reported the measured read range $d_{tag}$ = 1.8 m with the tag mounted on a metal surface. Although the information required for computing $d_{tag}$* is not provided, the reported measured radiation efficiency of 20% is notably higher than the 4.7% simulated for the folded T-matched dipole placed at the same distance from a metal plate in Section II.B. Moreover, the tag achieved similar performance in free space and on low-permittivity ($1\leq\varepsilon_r\leq4$) platforms.

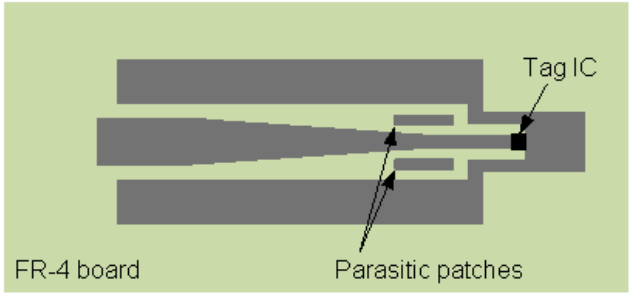


Figure 16. Fork-shaped antenna studied in [65].

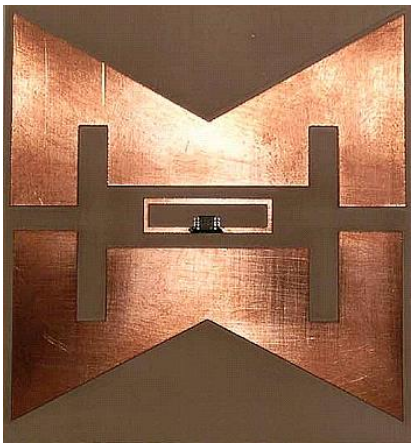

Figure 17. Double-bowtie antenna studied in [67].

The viability of dipole antennas for metal mountable tags was studied also in [67]. The authors achieved broadband characteristics by splitting a bow-tie element into two slightly dissimilar parts which are both proximity coupled to a feed loop carrying the tag IC. This antenna shape is shown in Fig. 17. The slight dissimilarity of the bow-tie elements manifested itself as a non-monotonic reactance frequency-response which provided bandwidth improvement. The simulated radiation efficiency and directivity of the antenna suspended on a 1.5 mm thick polytetrafluoroethylene (PTFE) –based substrate mounted on an infinite metal surface were 18% and 6.6 dBi, respectively. The tag has the overall size of $80.5\times74.5\times1.5$ mm$^3$ and it achieved the read range $d_{tag}$* = 11.2 m. In free space the read range dropped to around half of this.

Later, a similar antenna based on a single rectangular conductor strip as the main radiator was studied [68]. In this design the main radiator is proximity coupled to an inductive feed loop carrying the tag IC. The authors also proposed and validate an analytical framework for numerically efficient computation of the antenna impedance. Parametric study showed that the antenna resistance and reactance were controllable by varying the feed loop size and its separation from the patch, respectively. The patch shape determined the radiation properties of the antenna. The prototype tag has the

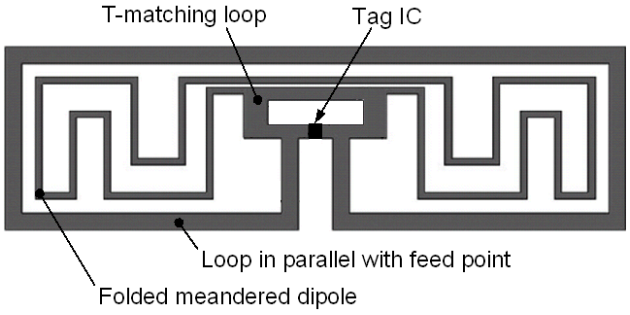


Figure 18. Folded meandered dipole studied in [69].

overall size of $118\times43\times1.5$ mm$^3$ and it achieved the read range $d_{tag}$* = 13.4 m when mounted on metal.

Continuation to the study of low-profile metal mountable tags based on dipole antennas was provided in [69], where the performances of folded meandered dipoles suspended on foam spacers of various thicknesses were evaluated. The authors found that an additional loop connected in parallel with the dipole feed point and enclosing the entire dipole structure provided gain improvements beyond 2 dB when the antenna was mounted on metal. The impedance tuning was done using T-matching approach. The prototype tag shown in Fig. 18 has the overall size of $91\times27\times h$ mm$^3$, where $h$ = 1 | 2 | 3 | 5 mm is the thickness of the foam spacer. The corresponding read range on metal is $d_{tag}$* = 6.7 | 9.1 | 11.4 | 13.4 m. The performance in free space was slightly better.

In the designs [67][68][69] discussed above, over 9 m read ranges were achieved with the antenna-metal separations up to 1.5 mm. However, as demonstrated in [70], much longer range is achievable in performance critical applications, where the slim form factor of the tag is not the top design priority. The studied antenna is a T-shaped slot with a narrow conductor strip going through the whole vertical section of the letter T. The tag IC was mounted over a gap in this strip and the antenna impedance was controlled by length of the current path around the T-slot. The antenna was patterned from copper on PET film, which was suspended on a 5-mm layer of foam. The prototype tag has the overall size of $125\times34\times5$ mm$^3$ and it achieved the read range $d_{tag}$* = 22.1 m when mounted on metal.

Regarding the size-performance ratio of the antennas without ground plane, the authors of [67][68][70] predicted that miniaturization would be obtained by using a high-permittivity substrate material. This miniaturization approach was investigated later in article [71] where a small slot antenna (Fig. 19) on ceramic Barium Titanate ($BaTiO_3$) substrate was presented. The relative permittivity and loss tangent of the substrate were estimated to be 39 and 0.02, respectively. The antenna has a circular footprint with the diameter of only 27.5 mm (0.09$\lambda$ at 915 MHz).

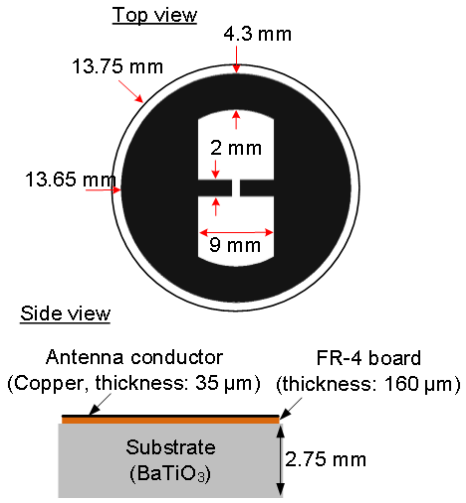


Figure 19. Slot antenna studied in [71].

While the use of high-permittivity materials is one of the well-known antenna miniaturization techniques and it has also been applied earlier in patch tags [55], for an antenna without ground plane, high-permittivity substrate increase the electrical separation between the antenna and metal surface. Moreover, in contrast to dipole types antennas discussed above, the authors of [71] considered the slot antenna to be advantageous in the application of metal mountable RFID tags for two reasons. Firstly, the comparison of a canonical slot and dipole structures within the same footprint showed that a stronger current is induced in the metal plate behind the dipole structure. This is illustrated in Fig. 20. Secondly, the input impedance of a slot antenna is inherently inductive below the antenna self-resonance frequency. This allows for conjugate impedance matching to capacitive tag ICs already below the antenna self-resonance frequency without additional matching structures.

The prototype antenna was patterned on a copper-clad FR-4 board (thickness: 0.16 mm) which was then mounted on ceramic $BaTiO_3$ substrate. The tag has the overall size of $27.5\text{Ø}\times2.9$ mm$^3$, where Ø denotes the diameter. Despite the

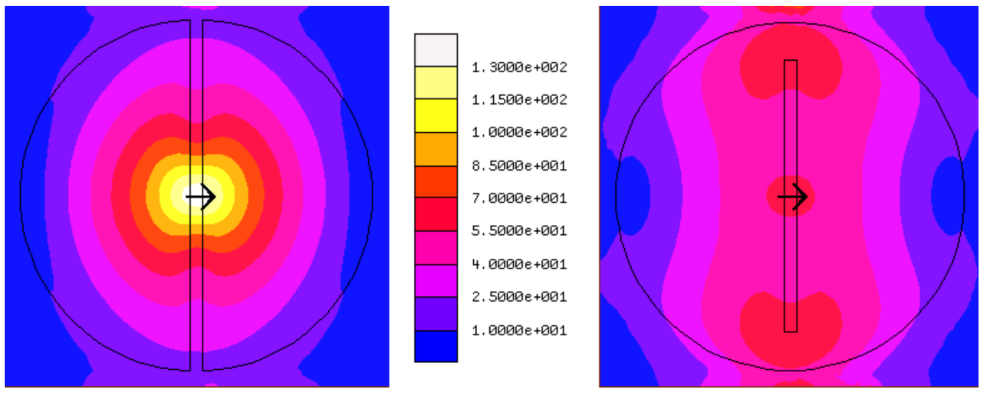


Figure 20. Surface current density [A/m] on metal plate beneath a dipole (on the left) and its complementary configuration (on the right) suspended on a 2.75 mm $BaTiO_3$ disk ($\varepsilon_r$=39, tan$\delta$=0.02) at 915 MHz. The antennas are accepting 100 mW.

Table 4. Comparison of metal mountable tags based on antennas without ground plane.

| Ref. | [65] | [67] | [68] | [69] | [70] | [71] | [72] |
|---|---|---|---|---|---|---|---|
| Tag size [mm$^3$] | $120\times30\times3.2$ | $80.5\times74.5\times1.5$ | $118\times43\times1.5$ | $91\times27\times1$ | $125\times34\times5$ | $27.5Ø\times2.9$ | $32Ø\times1.5$ |
| *ka* | 1.17 | 1.03 | 1.83 | 0.89 | 1.22 | 0.26 | 0.30 |
| Metal plate [cm$^2$] | $20\times20$ | $31\times23$ | $31\times23$ | NA | $20\times40$ | $20\times20$ | $10\times10$ |
| $d_{tag}$* [m] | 8.9 | 11.2 | 13.4 | 6.7 | 22.1 | 2.85 | 2.65 |
| Bandwidth | B | B | S | S | S | S | S |

S = single-band, B = broadband, W = wideband

$d_{tag}$* [m] is the reported tag read range referred to $P_{ic0}$ = −18 dBm and EIRP = 4 W under perfect polarization alignment.

slightly higher loss tangent of the ceramic substrate compared with conventional low-loss microwave circuit boards, the tag achieved the read range $d_{tag}$* = 2.85 m on metal. Importantly, over 1.2 m read range was maintained even on small metal plates with the sizes down to $3\times3$ cm$^2$. This verified the feasibility of the tag in the intended application: identification of *small* metallic items.

Although ceramic substrates can provide high dielectric constant, the rigid structure is not fit for all applications. However, flexible and high-permittivity polymer-ceramic composite materials provide compelling means for the development of small and conformal metal mountable tags. This approach was studied in [72], where the performance of a T-matched dipole antenna on flexible polymer-$BaTiO_3$ composite with the dielectric constant of 12 was characterized on both metallic plates and cylinders. The tag prototype shown in Fig. 21 has the overall size of $32Ø\times1.5$ mm$^3$ and it achieved the read range $d_{tag}$*= 2.65 m | 2.2 m when mounted on a metal plate | cylinder (radius: 35 mm). Importantly, the experimental and simulated characterizations showed that bending had little impact on the impedance matching. Increase in the plate size and reducing the cylinder radius improved the antenna directivity. This increased read range further.


Figure 21. Dipole antenna studied in [72].

Finally, Table 4 summarizes the performance of different metal mountable tags based on antennas without ground plane.

## V. Discussion and Future Prospects

Developing cheap, small, low-profile, and conformal antennas for RFID tags mountable on metallic objects presents a unique challenge. In the wireless communication systems, microstrip patch and planar inverted-F antennas are typically regarded as low-profile and compact structures. Since these antennas include a ground plane they benefit from the built-in tolerance toward the platform they are mounted on. These two aspects sparked initially the interest in developing metal mountable tags based on patch antennas and PIFAs.

As a result, antennas achieving high read ranges, up to 25 m, when mounted on metal plates were achieved and various techniques such as loading with slots and parasitic patches were successfully applied in size-reduction. However, the typically rigid and 2-to-3 mm thick structure of these antennas still limits their usage in RFID applications, where unobtrusive and flexible label type tags are needed. Nonetheless, in the identification and tracking of large and high-value assets, such as machinery, vehicles, and cargo containers, the metal mountable tags based on microstrip patch and planar inverted-F antennas are certainly a viable choice. On the other hand, for patch antennas in particular, progress has also been made toward thinner (less than 1 mm), smaller (footprint less than 10% the free space wavelength) and conformal structures, while combining all these desirable features in a single antenna is a topic of ongoing research.

The use of an EBG ground plane to enhance the performance of microstrip patch antennas through surface wave suppression has also been investigated. The in-phase reflection obtainable from an EBG surface has been employed in development of dipole antennas integrating an EBG surface to isolate it from the metallic object. However, further research on the miniaturization of the EBG structures is required to achieve EBG tags with size-performance ratios competitive against PIFA and patch tags.

Lately, the focus of the research on antennas for metal mountable RFID tags has been shifting from the antennas with ground planes toward structurally simpler designs based on a single conductor layer. These antennas hold the promise for

truly label type metal mountable tags fit for the identification and tracking of small everyday conductive items. As pointed out in Section IV, some of the tags based on single-layer antennas achieved high performance not only on metal, but also in free space and on low-permittivity platforms. This is an important aspect in the development toward universal tags, not exclusively designed for conductive items.

The major challenge in the design of single-layer antennas is to find effective means to reduce the currents induced in the conducting bodies in the antenna proximity. As discussed in Section II.B, this undesired antenna-metal interaction leads to various ailments, but perhaps the most prominent issue is the low radiation efficiency. Nonetheless, it has been shown that ad-hoc single-layer antennas suspended on foam spacers separating them from the conductive objects can achieve size-performance ratios similar to patch/PIFA tags. In addition, the foam-attached antennas benefit from the bendable and low-cost structure.

As opposed to foam spacers with low permittivity, flexible polymer-ceramic composite materials with high permittivity have also been found fit substrates for single-layer antennas in metal mountable tags. These materials are advantageous for two reasons: firstly, they increase the antenna-metal separation thus reducing the parasitic currents. Secondly, the high-permittivity material can be exploited in antenna miniaturization.

In the future, breakthroughs in the performance of single-layer antennas in the metal proximity are likely achieved through unconventional antenna design approaches, where insight on the antenna near fields is actively employed to adapt the antenna shape for minimal antenna-metal interaction. Another design approach, which is likely to improve the reliability of all metal mountable tags, is the thorough assessment of the impact of the shape and size of the conductive object on the antenna performance. Indeed, antennas backed by large conductive platforms tend to benefit from increased directivity, while in contrast, tags intended for the identification of small conductive may require antennas optimized considering the smallest conductive platform the tag can be mounted on. Moreover, optimizing the tag antennas toward broad spatial coverage for reliable power harvesting, instead of maximizing the peak read range, may prove to be the key in improving the overall reliability of the system.

## REFERENCES


[1] R. Want, "An Introduction to RFID Technology," *Pervasive Computing*, **5**, 1, January-March, 2006, pp. 25-33.

[2] K. Michael, J. McCathie, "The Pros and Cons of RFID in Supply Chain Management," International Conference on Mobile Business *Digest*, Sydney, Australia, July 11-13, 2005, pp. 623-629.

[3] J. Virtanen, L. Ukkonen, T. Björninen, A. Z. Elsherbeni, L. Sydänheimo, "Inkjet Printed Humidity Sensor for Passive UHF RFID Systems," *IEEE Transactions on Instrumentation and Measurement*, **60**, 8, August 2011, pp. 2768-2777.

[4] A. P. Sample, D. J. Yeager, P. S. Powledge, A. V. Mamishev, J. R. Smith, "Design of an RFID-based Battery-Free Programmable Sensing Platform," *IEEE Transactions on Instrumentation and Measurement*, **57**, 11, November 2008, pp. 2608-2615.

[5] R. Miesen, F. Kirsch, M. Vossiek, "Holographic Localization of Passive UHF RFID Transponders," IEEE International Conference on RFID *Digest*, Orlando, Florida, USA, April 12-14, 2011, pp. 32-37.

[6] M. Kim, N. Y. Chong, "Direction Sensing RFID Reader for Mobile Robot Navigation," *IEEE Transactions on Automation Science and Engineering*, **6**, 1, January 2009, pp. 44-54.

[7] G. Kortuem, F. Kawsar, D. Fitton, V Sundramoorthy, "Smart Objects as Building Blocks for the Internet of Things," *IEEE Internet Computing*, **14**, 1, January-February 2010, pp. 44-51.

[8] S. Roy, V. Jandhyala, J. R. Smith, D. J. Wetherall, B. P. Otis, R. Chakraborty, M. Buettner, D. J. Yeager, Y.-C. Ko, A. P. Sample, "RFID: From Supply Chains to Sensor Nets," *Proceedings of the IEEE*, **98**, 9, September 2010, pp. 1583-1592.

[9] L. Ukkonen, L. Sydänheimo, Y. Rahmat-Samii, "Sewed Textile RFID Tag and Sensor Antennas for on-Body Use," European Conference on Antennas *Digest*, Prague, Czech Republic, March 26-30, 2012, pp. 3450-3454

[10] C. Occhiuzzi, G. Marrocco, G, "The RFID Technology for Neurosciences: Feasibility of Limbs' Monitoring in Sleep Diseases," *IEEE Transactions on Information Technology in Biomedicine*, **14**, 1, January 2010, pp. 37-43.

[11] S. Merilampi, T. Björninen, L. Sydänheimo, L. Ukkonen, "Passive UHF RFID Strain Sensor Tag for Detecting Limb Movement," *International Journal of Smart Sensing and Intelligent Systems*, **5**, 2, June 2012, pp. 315-328.

[12] Z. Xiao, C.-M. Tang, C. M. Dougherty, R. Bashirullah, "A 20μW Neural Recording Tag with Supply-Current-Modulated AFE in 0.13μm CMOS," IEEE International Solid-State Circuits Conference *Digest*, San Francisco, California, USA, February 7-11, 2010, pp. 122-123.

[13] J. M. Rabaey, "Brain-Machine Interfaces as the New Frontier in Extreme Miniaturization," European Solid-State Circuits Conference *Digest*, Helsinki, Finland, September 19-24, 2011, pp. 19-24.

[14] C. A. Balanis, *Modern Antenna Handbook*, Hoboken, John Wiley & Sons, Inc., 2008.

[15] H.-W. Son, C.-S. Pyo, "Design of RFID Tag Antennas Using an Inductively Coupled Feed," *Electronics Letters*, **41**, 18, September 2005, pp. 994–996.

[16] G. Marrocco, "The Art of UHF RFID Antenna Design: Impedance-Matching and Size-Reduction Techniques," *IEEE Antennas and Propagation Magazine*, **50**, 1, February 2008, pp. 66-79.

[17] T. Björninen, A. Z. Elsherbeni, L. Ukkonen, "Performance of Single and Double T-Matched Short Dipole Tag Antennas for UHF RFID Systems," *Journal of Applied Computational Electromagnetics Society*, **26**, 12, June 2010, pp. 953-962.

[18] J. Xi, T. T. Ye, "Wideband and Material-Insensitive RFID Tag Antenna Design Utilizing Double-Tuning Technique," IEEE International Symposium on Antennas and Propagation *Digest*, Spokane, Washington, USA, July 3-8, 2011, pp. 545-548.

[19] E. Perret, S. Tedjini, R. S. Nair, "Design of Antennas for UHF RFID Tags," *Proceedings of the IEEE*, **100**, 7, July 2012, pp. 2330-2340.

[20] K. Mohammadpour-Aghdam, S. Radiom, R. Faraji-Dana, G. A. E. Vandenbosch, G. G. E. Gielen, "Miniaturized RFID/UWB Antenna Structure that can be Optimized for Arbitrary Input Impedance," *IEEE Antennas and Propagation Mag.*, **54**, 2, April 2012, pp. 74-87.

[21] G. De Vita, G. Iannaccone, "Design Criteria for the RF Section of UHF and Microwave Passive RFID Transponders," *IEEE Transactions on Microwave Theory and Techniques*, **53**, 9, September 2005, pp. 2978-2990.

[22] T. Björninen, M. Lauri, L. Ukkonen, R. Ritala, A. Z. Elsherbeni, L. Sydänheimo, "Wireless Measurement of RFID IC Impedance," *IEEE Transactions on Instrumentation and Measurement*, **60**, 9, September 2011, pp. 3194-3206.

[23] P. R. Foster, R. A. Burberry, "Antenna Problems in RFID Systems," IEE Colloquium on RFID Technology *Digest*, October 25, 1999, London, UK, pp. 3/1-3/5.

[24] J. D. Griffin, G. D. Durgin, A. Haldi, B. Kippelen, "RF Tag Antenna Performance on Various Materials Using Radio Link Budgets," *IEEE Antennas and Wireless Propagation Letters*, **5**, 1, December 2006, pp. 247-250.

[25] S. R. Aroor, D. D. Deavours "Evaluation of the State of Passive UHF RFID: an Experimental Approach," *IEEE Systems Journal*, **1**, 2, December 2007, pp. 168-176.
[26] S. R. Elliot, *Antenna Theory and Design*, An IEEE Classical Reissue, Hoboken, John Wiley & Sons, Inc., 2003.
[27] John D. Kraus, *Antennas*, New York, McGraw-Hill, Inc., 1988.
[28] P. Raumonen, L. Sydänheimo, L. Ukkonen, M. Keskilammi, M. Kivikoski, "Folded Dipole Antenna Near Metal Plate," IEEE International Symposium on Antennas and Propagation *Digest*, Columbus, Ohio, USA, June 22-27, 2003, pp. 848-851.
[29] J. Rashed, C.-T Tai, "A New Class of Resonant Antennas," *IEEE Transactions on Antennas Propagation*, **AP-39**, 9, September 1991, pp. 1428-1430.
[30] S. R. Best, J. D. Morrow, "On the Significance of Current Vector Alignment in Establishing the Resonant Frequency of Small Space-Filling Wire Antennas, " *IEEE Antennas and Wireless Propagation Letters*, **2**, 1, December 2003, pp. 201-204.
[31] A. Harmouch, H. A. Al Sheikh, "Miniaturization of the Folded-Dipole Antenna," *IEEE Antennas and Propagation Magazine*, **51**, 1, February 2009, pp. 117-123.
[32] T. Deleruyelle, P. Pannier, M. Egels, E. Bergeret, "An RFID Tag Antenna Tolerant to Mounting on Materials," *IEEE Antennas and Propagation Magazine*, **52**, 4, August 2010, pp. 14-19.
[33] Y. C. Or, K. W. Leung, R. Mittra, K. V. S. Rao, "Analysis on the Platform-Tolerant Radio-Frequency Identification Tag Antenna," *IET Microwaves, Antennas & Propagation*, **3**, 4, June 2009, pp. 601-606.
[34] H. Rajagopalan, Y. Rahmat-Samii, "Platform Tolerant and Conformal RFID Tag Antenna: Design, Construction and Measurements," *Journal of Applied Computational Electromagnetics Society*, **25**, 6, June 2010, pp. 486-497.
[35] J. H. Deng, W. S. Chan, B.-Z. Wang, S. Y. Zheng, K. F. Man, "An RFID Multicriteria Coarse- and Fine-Space Tag Antenna Design," *IEEE Transactions on Industrial Electronics*, **58**, 6, June 2011, pp. 2522-2530.
[36] M. A. Jensen, Y. Rahmat-Samii, "EM Interaction of Handset Antennas and a Human in Personal Communications," *Proceedings of the IEEE*, **83**, 1, January 1995, pp. 7-17.
[37] K. L. Virga, Y. Rahmat-Samii, "Low-Profile Enhanced-Bandwidth PIFA Antennas for Wireless Communications Packaging," *IEEE Transactions on Microwave Theory Techniques*, **45**, 10, October 1997, pp. 1879-1888.
[38] F. Yang, Y. Rahmat-Samii, *Electromagnetic Band Gap Structures in Antenna Engineering*, Cambridge, Cambridge University Press, 2009.

## Microstrip patch antennas for metal mountable tags

[39] L. Ukkonen, L. Sydänheimo, M. Kivikoski, "Patch Antenna with EBG Ground Plane and Two-Layer Substrate for Passive RFID of Metallic Objects," IEEE International Symposium on Antennas and Propagation *Digest*, Monterey, California, USA, 20-26 July, 2004, pp. 93-96.
[40] T. Björninen, K. Espejo Delzo, L. Ukkonen, A. Z. Elsherbeni, L. Sydänheimo, "Long Range Metal Mountable Tag Antenna for Passive UHF RFID Systems," IEEE International Conference on RFID-Technology and Applications *Digest*, Sitges, Spain, 15-16 September, 2011, pp. 194-198.
[41] H.-D. Chen, Y.-H. Tsao, C.-Y. Kuo, "Low-Profile Radio Frequency Identification Tag Antenna Using a Trapezoid Patch Mountable on Metallic Surfaces," *Microwave and Optical Technology Letters*, **52**, 8, August 2010, pp. 1697-1700.
[42] B. Yu, S.-J. Kim, B. Jung, F. J. Harackiewicz, B. Lee, "RFID Tag Antenna Using Two-Shorted Microstrip Patches Mountable on Metallic Objects," *Microwave and Optical Technology Letters*, **49**, 2, February 2007, pp. 414-416.
[43] S.-J. Kim, B. Yu, H.-J. Lee, M.-J. Park, F. J. Harackiewicz, B. Lee, "RFID tag antenna mountable on metallic plates," IEEE Asia-Pacific Microwave Conference *Digest*, Suzhou, China, December 4-7, 2005, Suzhou, China.
[44] S.-J. Kim, B. Yu, Y.-S. Chung, F. J. Harackiewicz, B. Lee, "Patch Type Radio Frequency Identification Tag Antenna Mountable on Metallic Platforms," *Microwave and Optical Technology Letters*, **48**, 12, December 2006, pp. 2446-2448.
[45] B. Lee, B. Yu, "Compact Structure of UHF Band RFID Tag Antenna Mountable on Metallic Objects," *Microwave and Optical Technology Letters*, **50**, 1, January 2008, pp. 232-234.
[46] L. Mo, H. Zhang, H. Zhou, "Broadband UHF RFID Tag Antenna with a Pair of U Slots Mountable on Metallic objects," *Electronics Letters*, **44**, 20, September 2008, pp. 1173-1174.
[47] M.-Y. Lai, R.-L. Li, "A Low-Profile Broadband RFID Tag Antenna for Metallic Objects," International Conference on Microwave and Millimeter Wave Technology *Digest*, Chengdu, China, May 8-11, 2010, pp. 1891-1893.
[48] T. V. Koskinen, H. Rajagopalan, Y. Rahmat-Samii, "A Thin Multi-Slotted Dual Patch UHF-band Metal-Mountable RFID Tag Antenna," *Microwave and Optical Technology Letters*, **53**, 1, October 2011, pp. 40-47.
[49] S.-L. Chen, K. H. Lin, "A Slim RFID Tag Antenna Design for Metallic Object Applications," *IEEE Antennas and Wireless Propagation Letters*, **7**, 1, December 2008, pp. 729-732.
[50] S.-L. Chen, "A Miniature RFID Tag Antenna Design for Metallic Objects Application," *IEEE Antennas and Wireless Propagation Letters*, **8**, 1, December 2009, pp. 1043-1045.
[51] S.-L. Chen, R. Mittra, "A Long Read Range RFID Tag Design for Metallic Objects," European Conference on Antennas and Propagation *Digest*, Barcelona, Spain, April 12-16, 2010, 3 p.
[52] M.-Y. Lai, R.-L. Li, M. M. Tentzeris, "Low-Profile Broadband RFID Tag Antennas Mountable on Metallic Objects," IEEE International Symposium on Antennas and Propagation *Digest*, July 11-17, 2010, Toronto, Ontario, Canada, 4 p.
[53] J. Z. Huang, P. H. Yang, W. C. Chew, T. T. Ye, "A Novel Broadband Patch Antenna for Universal UHF RFID Tags," *Microwave and Optical Technology Letters*, **52**, 12, December 2010, pp. 2653-2657.
[54] H.-W. Son, S.-H. Jeong, "Wideband RFID Tag Antenna for Metallic Surfaces Using Proximity-Coupled Feed," *IEEE Antennas and Wireless Propagation Letters*, **10**, 1, December 2011, pp. 377-380.
[55] J.-S. Kim, W.-K. Choi, G.-Y. Choi, "Small Proximity Coupled Ceramic Patch Antenna for UHF RFID Tag mountable on Metallic Objects," *Progress in Electromagnetics Research C*, **4**, 2008, pp. 129-138.

## Planar inverted-F antennas for metal mountable tags

[56] L. Ukkonen, D. Engels, L. Sydänheimo, M. Kivikoski, "Planar Wire-Type Inverted-F RFID Tag Antenna Mountable on Metallic Objects," IEEE International Symposium on Antennas and Propagation *Digest*, Monterey, California, USA, July 20-26, 2004, pp. 101-104.
[57] M. Hirvonen, P. Pursula, K. Jaakkola, K. Laukkanen, "Planar Inverted-F Antenna for Radio Frequency Identification," *Electronics Letters*, **40**, 14, July 2004, pp. 848-850.
[58] H. Kwon, B. Lee, "Compact Slotted Planar Inverted-F RFID Tag Mountable on Metallic Objects," *Electronics Letters*, **41**, 24, November 2005, pp. 1308-1310.
[59] M. Hirvonen, K. Jaakkola, P. Pursula, J. Säily, "Dual-Band Platform Tolerant Antennas for Radio-Frequency Identification," *IEEE Transactions on Antennas and Propagation*, **AP-54**, 9, September 2006, pp. 2632-2637.
[60] W. Choi, H. W. Son, J.-H. Bae, G. Y. Choi, C. S. Pyo, J.-S. Chae, "An RFID Tag Using a Planar Inverted-F Antenna Capable of Being Stuck to Metallic Objects," *ETRI Journal*, **28**, 2, April 2006, pp. 216-218.
[61] L. Mo, C. Qin, "Tunable Compact UHF RFID Metal Tag Based on CPW Open Stub Feed PIFA Antenna," *International Journal on Antennas and Propagation*, **2012**, December 2012, article ID 167658, 8 p.

## Antennas integrating EBG for metal mountable tags

[62] L. Ukkonen, L. Sydanheimo, M. Kivikoski, "Effects of Metallic Plate Size on the Performance of Microstrip Patch Type Tag Antennas for Passive RFID," *IEEE Antennas and Wireless Propagation Letters*, **4**, 1, December 2005, pp. 410-413.
[63] D.-U. Sim, D.-H. Kim, J.-I. Choi, H.D. Choi, "Design of Novel Dipole Type Tag Antennas Using Electromagnetic Bandgap (EBG) Surface for Passive RFID Applications," IEEE International Symposium on Antennas and Propagation *Digest*, Honolulu, Hawaii, USA, June 9-15, 2007, pp. 1333-1336.
[64] B. Gao, M. M. F. Yuen, "Passive UHF RFID Packaging with Electromagnetic Band Gap (EBG) Material for Metallic Objects

Tracking," *IEEE Transactions on Components and Packaging Technology*, **1**, 8, August 2011, pp. 1140-1146.

Antennas without a ground plane for metal mountable tags

[65] K.-H. Kim, J.-G. Song, D.-H. Kim, H.-S. Hu, J.-H. Park, "Fork-Shaped RFID Tag Antenna Mountable on Metallic Surfaces," *Electronics Letters*, **43**, 25, December 2007, pp. 1400-1402.

[66] C. Cho, H. Choo, I. Park, "Design of Planar RFID Tag Antenna for Metallic Objects," *Electronics Letters*, **44**, 3, January 2008, pp. 175-177.

[67] J. Dacuna, R. Pous, "Low-Profile Patch Antenna for RF Identification Applications," *IEEE Transactions on Microwave Theory and Techniques*, **57**, 5, May 2009, pp. 1406-1410.

[68] S.-K. Kuo, L.-G. Liao "An Analytic Model for Impedance Calculation of an RFID Metal Tag," *IEEE Antennas and Wireless Propagation Letters*, **9**, 1, December 2010, pp. 603-607.

[69] T.-W. Koo, D. Kim, J.-I. Ryu, H.-M. Seo, J.-G. Yook, J.-C. Kim, "Design of a Label Typed UHF RFID Tag Antenna for Metallic Objects," *IEEE Antennas and Wireless Propagation Letters*, **10**, 1, December 2011, pp. 1010-1014.

[70] Y. Park, J. N. Lee, J. K. Park, "Design of UHF Radio Frequency Identification Metal Tag Antenna Using T-shaped Slot," *Microwave and Optical Technology Letters*, **53**, 10, October 2011, pp. 2251-2255.

[71] T. Björninen, A. A. Babar., A. Z. Elsherbeni, L. Ukkonen, L. Sydänheimo, J. Kallioinen, "Compact metal mountable UHF RFID tag on a Barium Titanate based substrate," *Progress in Electromagnetics Research C*, **26**, 2012, pp. 43-57.

[72] A. A. Babar., T. Björninen, V. A. Bhagavati, L. Sydänheimo, P. Kallio, L. Ukkonen, "Small and Flexible Metal Mountable Passive UHF RFID Tag on High Dielectric Ceramic-Polymer Composite Substrate," *IEEE Antennas and Wireless Propagation Letters*, **11**, 1, December 2012, pp. 1319-1323.

**Toni Björninen** was born 1984. He received the M.Sc. and Ph.D. degrees with distinction in electrical engineering both from Tampere University of Technology (TUT), Tampere, Finland, in 2009 and 2012, respectively. He is currently a Research Fellow in the Wireless Identification and Sensing Systems Research Group at the TUT Department of Electronics and Communications Engineering, Rauma Research Unit. He has authored over 50 scientific publications on antennas for RFID and biomedical systems. His research interests are focused on implantable and wearable antennas, RFID, and modeling of electromagnetics.

**Lauri Sydänheimo** received the M.Sc. and Ph.D. degrees in electrical engineering from Tampere University of Technology (TUT), Tampere, Finland. He is currently a Professor and Head of the Department of Electronics and Communications Engineering, TUT, and is the Research Director of the Rauma Research Unit of Department of Electronics and Communications Engineering, TUT. He has authored over 170 publications in the field of RFID tag and reader antenna design and RFID system performance improvement. His research interests are focused on wireless data communication and radio frequency identification (RFID), particularly RFID antennas and sensors.

**Leena Ukkonen** received the M.Sc. and Ph.D. degrees in electrical engineering in 2003 and 2006, respectively. She is currently a Professor at the TUT Department of Electronics and Communications Engineering, and is leading the Wireless Identification and Sensing Systems Research Group at the TUT Department of Electronics and Communications Engineering, Rauma Research Unit. She is Academy of Finland Research Fellow and holds Adjunct Professorship in Aalto University School of Science and Technology, Espoo, Finland. She has authored over 130 scientific publications in the fields of RFID antenna design and industrial RFID applications. Her research interests are focused on RFID antenna development for tags, readers and RFID sensors.

**Yahya Rahmat-Samii** is a Distinguished Professor, holder of the Northrop Grumman Chair in Electromagnetics, member of the US National Academy of Engineering (NAE) and past Chairman of the Electrical Engineering Department, University of California, Los Angeles (UCLA). He was a Senior Research Scientist with the National Aeronautics and Space Administration (NASA) Jet Propulsion Laboratory (JPL), California Institute of Technology prior to joining UCLA in 1989. In summer 1986, he was a Guest Professor with the Technical University of Denmark (TUD). He has also been a consultant to numerous aerospace and wireless companies. He has been Editor and Guest editor of numerous technical journals and books. He has authored and coauthored over 800 technical journal and conference papers and has written 30 book chapters. He is a coauthor of Electromagnetic Band Gap Structures in Antenna Engineering (New York: Cambridge, 2009), Implanted Antennas in Medical Wireless Communications (Morgan & Claypool Publishers, 2006), Electromagnetic Optimization by Genetic Algorithms (New York: Wiley, 1999), and Impedance Boundary Conditions in Electromagnetics (New York: Taylor & Francis, 1995). He has received several patents. He has had pioneering research contributions in diverse areas of electromagnetics, antennas, measurement and diagnostics techniques, numerical and asymptotic methods, satellite and personal communications, human/antenna interactions, RFID and implanted antennas in medical applications, frequency selective surfaces, electromagnetic band-gap structures, applications of the genetic algorithms and particle swarm optimization, etc., (visit http://www. antlab.ee.ucla.edu/).

Dr. Rahmat-Samii is a Fellow of the Institute of Advances in Engineering (IAE) and a member of Commissions A, B, J and K of USNC-URSI, the Antenna Measurement Techniques Association (AMTA), Sigma Xi, Eta Kappa Nu and the Electromagnetics Academy. He was Vice-President and President of the IEEE Antennas and Propagation Society in 1994 and 1995,

respectively. He was appointed an IEEE AP-S Distinguished Lecturer and presented lectures internationally. He was a member of the Strategic Planning and Review Committee (SPARC) of the IEEE. He was the IEEE AP-S Los Angeles Chapter Chairman (1987-1989); his chapter won the best chapter awards in two consecutive years. He is listed in Who's Who in America, Who's Who in Frontiers of Science and Technology and Who's Who in Engineering. He has been the plenary and millennium session speaker at numerous national and international symposia. He has been the organizer and presenter of many successful short courses worldwide. He was a Directors and Vice President of AMTA for three years. He has been Chairman and Co-chairman of several national and international symposia. He was a member of the University of California at Los Angeles (UCLA) Graduate council for three years. He was the chair of USNC-URSI for the period of 2009-2011.

For his contributions, Dr. Rahmat-Samii has received numerous NASA and JPL Certificates of Recognition. In 1984, he received the Henry Booker Award from URSI, which is given triennially to the most outstanding young radio scientist in North America. Since 1987, he has been designated every three years as one of the Academy of Science's Research Council Representatives to the URSI General Assemblies held in various parts of the world. He was also invited speaker to address the URSI 75th anniversary in Belgium. In 1992 and 1995, he received the Best Application Paper Prize Award (Wheeler Award) for papers published in 1991 and 1993 IEEE Transactions on Antennas and Propagation. In 1999, he received the University of Illinois ECE Distinguished Alumni Award. In 2000, Prof. Rahmat-Samii received the IEEE Third Millennium Medal and the AMTA Distinguished Achievement Award. In 2001, Rahmat-Samii received an Honorary Doctorate in applied physics from the University of Santiago de Compostela, Spain. In 2001, he became a Foreign Member of the Royal Flemish Academy of Belgium for Science and the Arts. In 2002, he received the Technical Excellence Award from JPL. He received the 2005 URSI Booker Gold Medal presented at the URSI General Assembly. He is the recipient of the 2007 Chen-To Tai Distinguished Educator Award of the IEEE Antennas and Propagation Society. In 2008, he was elected to the membership of the US National Academy of Engineering (NAE). In 2009, he was selected to receive the IEEE Antennas and Propagation Society highest award, Distinguished Achievement Award, for his outstanding career contributions. He is the recipient of the 2010 UCLA School of Engineering Lockheed Martin Excellence in Teaching Award, the 2011 UCLA Distinguished Teaching Award and the 2011 IEEE Electromagnetics Award. Prof. Rahmat-Samii is the designer of the IEEE AP-S logo which is displayed on all IEEE AP-S publications.

### *Fundamentals of Passive UHF RFID Systems*

The core components and operation principles of passive UHF RFID systems are illustrated in Fig. A.1. The use of the modulated antenna scattering as a means for wireless communication was introduced as early as 1948 [A.1]. One of the first completely passive RFID tags was reported in 1975 [A.2], but it was not until the successful fabrication of Schottky diodes on a regular CMOS integrated circuit in 1990's that the passive RFID tags started to assume their present shape without off-chip components, other than the antenna. With this development, the design of fully integrated RFID ICs got into full speed and correspondingly, a great amount of research on antennas for the passive tags has been done during the past decade. [A.3]

Referring to Fig. A.1, passive RFID tags consist of only two separate entities: the tag antenna and the RFID tag microchip (tag IC). The passive tags are remotely powered by the reader and the tag-to-reader data link is based modulated antenna scattering. The communication by means of reflected power provides superior power efficiency on the tag side compared with active transmission. As a result, the reader can interrogate the battery-free tags from the distances of several meters. With specialized tag antennas distances beyond 20 meters can be achieved.

The tag antenna, is responsible for capturing energy from the continuous wave emitted by the reader. The tag antenna radiation efficiency describes the power efficiency in this process while the tag antenna directivity measures the antenna's ability to extract power from an incident electromagnetic wave impinging on it from a certain direction. Finally, the antenna-IC power transfer efficiency (determined by the antenna and tag IC impedances) identifies the fraction of the captured power that is being delivered to the tag IC [A.4]. These are the three fundamental tag performance indicators on which the tag designer needs to focus on.

Once there is sufficient voltage across the antenna terminals to activate the semiconductor devices in the on-chip rectifier, it starts to supply power to wake up the rest of the circuit. With the tag IC fully activated, the on-chip radio listens in for commands from the reader, but the tag never responds to the reader spontaneously. The reader may also request new data to be recorded in the on-chip memory, but in the most common operation cycle, the reader polls for the identification code of the tag stored in the memory. The tag responds by modulating the requested information in the scattering from the tag antenna using the on-chip impedance switching scheme. Once the response is detected by the reader, the identification data is distributed over to the data management system. [A.5]

Due to the abundance of the wireless systems, the radio spectrum has been divided into sub-bands with regulated emission limits to keep the inter-system interference at a tolerable level. In practice, the emission limit is imposed as the equivalent isotropically radiated power (EIRP), defined as the product of the power accepted by the transmit antenna and its maximum gain over all the spatial angles within the regulated frequency band. This enforces the same maximum radiated power density for any transmitting antenna. In addition to the performance of the tag antenna and the EIRP regulation, the readable of an RFID tag depends on the tag IC wake-up power ($P_{ic0}$). Thus, it is important to always refer the achieved read range to a specific EIRP value and $P_{ic0}$ in order to establish a judicious performance comparison between different tag antenna designs.

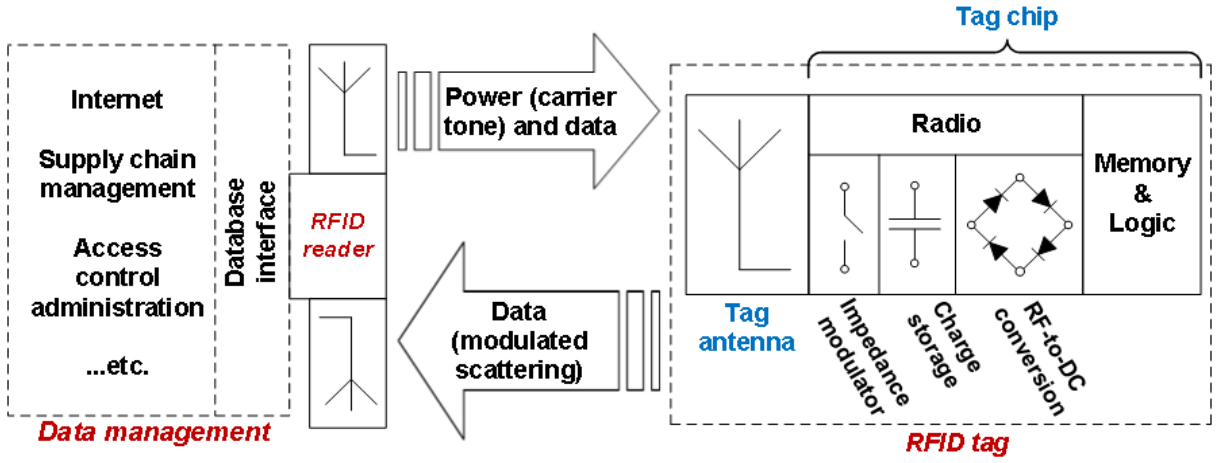


Fig. A.1. The core components and operation principle of passive UHF RFID systems.

Communication protocols for RFID are also being standardized. Currently, there is ISO 18000-6 standard [A.6] defining the air interface protocol for RFID. In addition, the most widely used tags follow EPCglobal UHF Class 1 Generation 2 standard [A.7], which defines the physical and logical requirements for the tags. Currently, UHF RFID systems are operated within the regionally regulated sub-bands of the global frequency range of 840–960 MHz. For instance, the frequency range of 865.6–867.6 MHz is used in Europe, 902–928 MHz in Canada and U.S. while in some countries, e.g. in China, Japan and Korea, there are multiple bands available with different power transmission regulations while new bands around the world are opening all the time [A.7].

***References***


[A.1] H. Stockman, ”Communication by Means of Reflected Power,” *Proceedings of the IRE*, **36**, 10, October 1948, pp. 1196-1204.

[A.2] A. R. Koelle, S. W. Depp, R. W. Freyman, ”Short-Range Radio-Telemetry for Electronic Identification, Using Modulated RF Backscatter,” *Proceedings of the IEEE*, **63**, 8, August 1975, pp. 1260-1261.

[A.3] J. Landt, ”The history of RFID,” *IEEE Potentials*, **24**, 4, October-November 2005, pp. 8-11.

[A.4] G. Marrocco, ”The Art of UHF RFID Antenna Design: Impedance-Matching and Size-Reduction Techniques,” *IEEE Antennas and Propagation Magazine*, **50**, 1, February 2008, pp. 66-79.

[A.5] D. Dobkin, *The RF in RFID: Passive UHF RFID in Practice*, Burlington, Newnes-Elsevier, Inc., 2008.

[A.6] International Organization for Standardization, ISO/IEC 18000-6, www.iso.org/

[A.7] EPCglobal, Overview of the ultra high frequency (UHF) regulations worldwide, http://www.gs1.org/epcglobal/implementation